



## FLOW OF CONCENTRATED NON-NEWTONIAN SLURRIES: 2. FRICTION LOSSES IN BENDS, FITTINGS, VALVES AND VENTURI METERS

R. M. TURIAN†, T.-W. MA‡, F.-L. G. HSU§, M D.-J. SUNG¶  
and G. W. PLACKMANN||

Department of Chemical Engineering, 810 S. Clinton Street, University of Illinois at Chicago, Chicago, IL 60607, U.S.A.

(Received 22 August 1996; in revised form 15 May 1997)

**Abstract**—Friction losses for the flow of concentrated slurries of laterite and gypsum through 2.5 and 5.0 cm bends, fittings, valves and Venturi meters were determined. The experimental work was carried out using a slurry flow facility consisting of several flow loops throughout which the different piping elements had been installed. The friction losses for each piping element are based on detailed measurements of the axial pressure distributions along the element including that along upstream and downstream tangent lines consisting of long sections of straight pipe of the same diameter. Pressure losses for the fully-developed flow through straight pipe test sections were also measured to use as baselines. For flow through 45° and 180° bends, 90° bends of different radii of curvature, and gate and globe valves, resistance coefficients, based on slurry density, were found to be inversely proportional to the generalized Reynolds number for laminar flow, and to approach constant asymptotic values for turbulent flow. The latter were the same as the high-Reynolds number limiting values for flow of water through the respective fitting. Correlations for resistance coefficients for slurry flow through concentric 5.0 × 2.5 cm<sup>2</sup> sudden contraction and 2.5 × 5.0 cm<sup>2</sup> sudden enlargement were also established. Discharge coefficients for flow of slurries and water through 2.5 and 5.0 cm Venturi meters with throat to pipe diameter ratios of 0.5 and 0.75 were also determined. For slurries the discharge coefficients increased with increasing flow rate and approached asymptotic values at high flow rates which were the same as the values for highly turbulent flow of water. © 1998 Elsevier Science Ltd. All rights reserved

**Key Words:** non-Newtonian slurries, flow through bends, valves, Venturi meters, resistance coefficients, discharge coefficients

### 1. INTRODUCTION

Pressure losses for the flow of concentrated mineral slurries of laterite and gypsum through an array of piping elements were measured. Altogether data on a total number of 24 different piping elements were taken. These consisted of 2.5 and 5.0 cm diameter sizes of each of the following: 45° bends (2), 180° return bends (2), 90° bends in five different radius of curvature to pipe diameter ratios (10), gate and globe valves (4), Venturi meters in two different throat to pipe diameter ratios (4), and a 2.5 × 5.0 cm<sup>2</sup> concentric sudden enlargement and a 5.0 × 2.5 cm<sup>2</sup> concentric sudden contraction (2). A critical experimental investigation on such a large array of piping elements is a rather major undertaking. This is not only because it is necessary to collect a lot of data for each fitting to insure that broad enough ranges of Reynolds numbers and slurry concentrations have been covered, but also because for each flow rate multiple pressure drop measurements must be taken to establish detailed information on axial pressure gradients along the upstream as well as the downstream tangent lines connecting the piping element to the flow system. Almost no published information on friction losses for the flow of non-Newtonian fluids or fine particulate and colloidal suspensions through flow disturbances is available, and what little exists is rather

†To whom all correspondence should be addressed.

‡Present address: NOXSO Corp., Library, PA 15129, U.S.A.

§Present address: Lever Bros., Edgewater, NJ 07020, U.S.A.

¶Present address: Yeungnam University, Kyongsan 712-749, South Korea.

||Present address: Johnson Controls Inc., Geneva, IL 60134, U.S.A.

sparse. We have published the results of an extensive study on friction losses for the flow of coarse-particle slurries through arrays of piping elements in the past (Turian *et al.* 1983), but these involved noncolloidal, settling slurries of narrow-sized glass beads in water. As nonuniform, non-continuum dispersed systems, these slurries were neither amenable to rheological measurement nor to classification.

### 1.1. *Classification of piping elements and flow disturbances*

Pressure losses in piping systems result from wall friction, changes in direction of the flow, obstructions in the flow path, and sudden or gradual changes in cross-section or shape of the flow duct. Pipe fittings may be classified as branching, reducing, expanding or deflecting types. Reducers, bushings, enlargements and contractions are fittings which change the area of the flow passage and belong to the reducing or expanding class of fittings. Elbows, bends, return bends and other fittings which cause a change in the direction of the flow are of the deflecting type. Aside from these there are a number of fittings and piping elements which possess combinations of the attributes of the general classes enumerated here, and also types, such as couplings and unions, which ordinarily present little resistance to the flow.

The literature on Newtonian flow through piping systems and pipeline transitions is extensive, and embodies experimental and theoretical studies as well as extensive tabulations of resistance coefficients and empirical correlations. We will present a review of some pertinent parts of this published work because it provides guides to our present studies, and because friction losses for Newtonian flows constitute references against which losses for non-Newtonian flows through complex geometries are measured.

The presence of a fitting usually results in disturbance to the flow, and this is manifested by a friction loss in excess of that attributable to flow through a straight pipe segment having the same physical path length. It is not possible to isolate a fitting within a piping system, and therefore it is not possible to measure directly the friction losses solely attributable to it. The disturbance resulting from the presence of a fitting affects the flow upstream as well as that downstream of the fitting; the downstream effect usually projecting over a longer segment of connecting piping. To obtain data capable of unambiguous accounting for the friction losses associated with the connecting piping, and thereby to establish the reference for calculating the correct friction loss due to the fitting alone, both upstream and downstream straight pipe sections, or so-called tangent lines, must be long enough to insure that fully developed flow exists at least at some point within the connecting straight pipes. It is not enough to measure the pressure drop merely across the disturbance itself. Indeed, for each flow rate it is necessary to measure the variation of the axial pressure drop along the upstream as well as the downstream tangent lines, in order to establish the lengths of connecting tangent lines affected by the disturbance, and by how much.

### 1.2. *Friction losses in fittings—the macroscopic balances*

Our reference for accounting for the various losses in a piping system is the steady state macroscopic mechanical energy balance, which under isothermal conditions, and no work involved, is given by (Bird *et al.* 1960)

$$(P_1/\rho_1) + (gZ_1) + (V_1^2/2) = (P_2/\rho_2) + (gZ_2) + (V_2^2/2) + h_f. \quad [1]$$

The subscript 1 designates the position upstream and 2 the position downstream of the fitting, and  $h_f$  is the friction loss per unit mass of fluid. Strictly, the velocity head terms in [1] should include kinetic energy correction factors to account for possible non-flat velocity profiles at sections 1 and 2. This equation applies to Newtonian and non-Newtonian fluids and to suspensions.

For the steady flow of an incompressible fluid through a section of circular pipe of diameter  $D$  and length  $L$ , lying in a horizontal plane so that  $Z_1 = Z_2$ , we have  $V_1 = V_2 = V$ , and [1] gives

$$h_f = (P_1 - P_2)/\rho = (V^2/2)[4(L/D)f] \quad [2]$$

in which the friction factor is defined by

$$f = \tau_w/(\rho V^2/2) = [(-\Delta P/L)(D/4)]/(\rho V^2/2). \quad [3]$$

A typical experimental assembly surrounding a fitting, such as a bend or valve, lying in a

horizontal plane with its connecting tangent lines is represented schematically in figure 1. The axial pressure profile along this section of pipe is also given in this diagram. As explained below, fittings which result in change of cross-section, and piping sections which do not lie entirely in a horizontal plane, can also be subsumed within this scheme provided the total head, instead of merely the pressure, is plotted in the diagram. In figure 1 the curve ABCD represents the axial pressure profile between upstream and downstream pressure taps for the piping section containing the disturbance, and the curve AB'C'D' represents the profile for the case when the fitting is replaced by a continuous section of straight pipe. If the fitting were removed altogether there would be no loss for the section of piping corresponding to its actual physical length, and the pressure profile would follow the curve AB'C'D". It should be observed that the slope of the line segment AB', which gives the pressure gradient along the upstream tangent undisturbed by the presence of the fitting (where the flow enters as fully-developed), is the same as the slope of the line segment ED, to which the axial pressure curve ABCD asymptotically tends. Thus, the downstream station 2 is taken at a point where the effect of the fitting is no longer felt, and the flow has reverted to fully-developed conditions.

According to figure 1 the overall pressure drop caused by the disturbance consists of three contributions.

- (1) The pressure drop in the piping upstream of the disturbance in excess of that which would occur in the absence of the fitting; given by  $(-\Delta P)_u$  or BB'. This effect is usually small and results from propagation of the disturbance upstream of the piping element.
- (2) The pressure drop within the disturbance itself; given by  $(-\Delta P)_o$  or BC.
- (3) The pressure drop in the piping downstream of the disturbance in excess of that which would occur in the absence of the fitting; given by  $(-\Delta P)_d$  or CE. This effect is comparatively large; the effect of the disturbance is projected over a longer distance in the downstream flow before fully-developed flow conditions are re-established.

It is not easy to measure each of these pressure drops separately, nor is it necessary, as the combined effect is what is usually of interest. The total pressure loss chargeable to the disturbance is given by

$$(-\Delta P)_t = (-\Delta P)_u + (-\Delta P)_o + (-\Delta P)_d. \tag{4}$$

The total pressure drop given by [4] includes the contribution due to the actual length of the fitting.

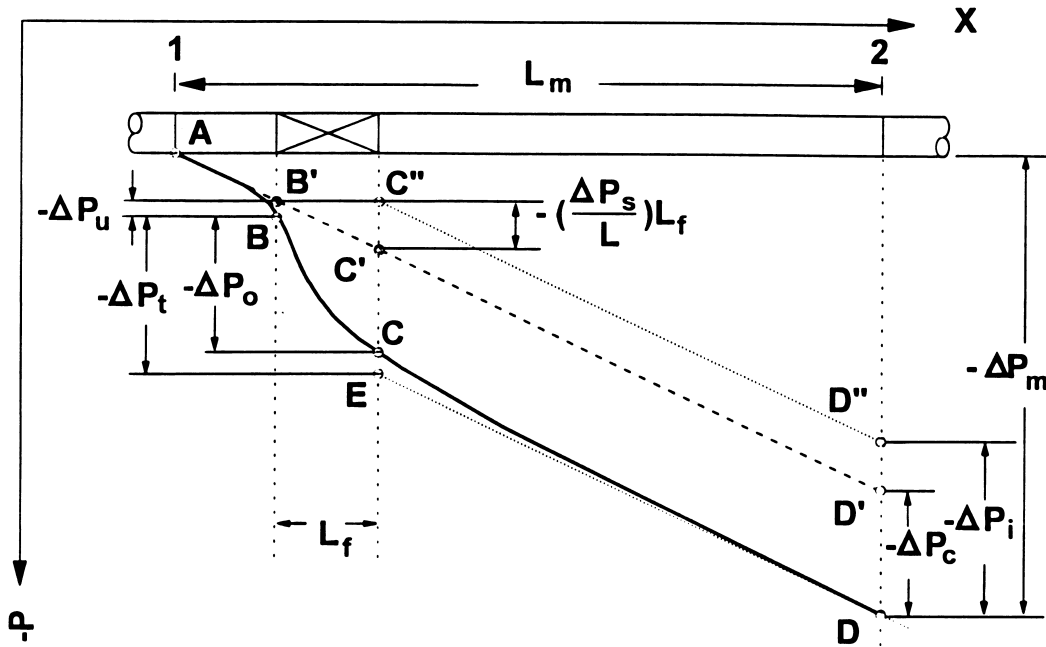


Figure 1. Typical axial pressure profile along piping system containing a fitting.

$(-\Delta P)_i$  is also designated as  $(-\Delta P)_i$ . An alternative expression of the pressure loss due to a fitting is one which excludes the contribution due to the actual physical length of the fitting. This 'corrected' pressure drop is designated by  $(-\Delta P)_c$ . These are shown in figure 1. The quantity  $(-\Delta P_s/L)$  is the pressure gradient for fully-developed flow of the suspension through the straight pipe.

For fittings resulting in change of cross-sectional area of the flow there is a conversion of velocity head to pressure head (expansions) and the reverse (contractions). Further, if the piping section containing the disturbance does not lie wholly in the same horizontal plane, the contribution due to changes in potential energy must be included. Taking conditions at the upstream section 1 as the reference, and designating the distance along the axis of the piping section from the reference point 1 by  $x$ , we have from [1]

$$h_f(x) = -(1/\rho)[P(x) - P_1] - g[Z(x) - Z_1] - (1/2)[V^2(x) - V_1^2]. \quad [5]$$

Accordingly, for piping sections in which changes in cross-section and/or elevation are present, the total head,  $h_f(x)$ , must be plotted against  $x$  in figure 1.

As shown in figure 1 the flow is fully developed at the upstream (1) and downstream (2) sections, and the experimentally measured pressure drop between these two points is  $(-\Delta P)_m$ . The total pressure drop across the fitting and that corrected for the physical length of the fitting are given, respectively, by,

$$(-\Delta P)_i = (-\Delta P)_m - (-\Delta P_s/L)(L_m - L_f) \quad [6]$$

$$(-\Delta P)_c = (-\Delta P)_m - (-\Delta P_s/L)L_m. \quad [7]$$

### 1.3. Friction losses, resistance coefficients and equivalent length

Friction losses for fittings are expressed in terms of the so-called *resistance coefficients*  $K$  defined by

$$K = h_f/(V^2/2). \quad [8]$$

Alternatively, the friction loss can be expressed in terms of the equivalent length of straight pipe of the same diameter and having the same friction loss as the fitting. The equivalent length is expressed in numbers of pipe diameters,  $(L_e/D)$ , and is obtained by equating friction loss terms from [2] with that from [8]:

$$(L_e/D) = K/4f. \quad [9]$$

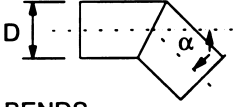
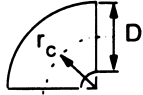
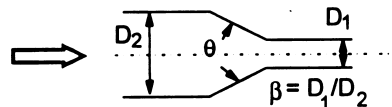
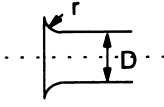
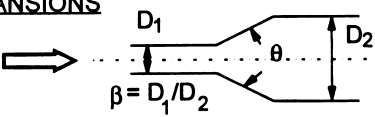
It can be shown, using dimensional analysis, that for incompressible Newtonian fluids  $K$  is a dimensionless function of  $Re$  and of dimensionless geometric ratios characteristic of the fitting or valve:

$$K = f\eta \text{ (Re, geometric ratios)}. \quad [10]$$

[10] suggests that the resistance coefficient is the same for all sizes of a given type of fitting provided dynamic similarity is enforced, i.e. equality of Reynolds number and geometric similarity are maintained. It is found, however, that  $K$  is usually not strongly dependent on  $Re$  since, as in turbulent pipe flow,  $h_f$  is nearly proportional to  $V^2$ . Furthermore, economic considerations and constraints dictated by requirements of standards and structural strength preclude fabrication of strictly geometrically similar fittings and valves in the different sizes of any given design.

A very extensive tabulation of resistance coefficients for turbulent flow through a broad variety of piping elements has been compiled by the Crane Company (1980). Table 1 presents a concise selection of typical approximate values of resistance coefficients for turbulent flow through various types and sizes of fittings. The  $K$  values in this table include the contribution due to the actual physical length of the fitting, and are clearly to be viewed as typical approximate values. The actual value of the friction loss in any given instance will depend upon the particular design of the fitting of any given type, its condition of wear, and its internal surface roughness.

Table 1. Resistance coefficients for turbulent flow through various fittings

Resistance Coefficient: $K = N \lambda_T$														
Friction Factor, $\lambda_T$ , for Clean Commercial Steel Pipe in Fully-Developed Turbulent Flow														
Nominal Size	1/2"	3/4"	1"	1 1/4"	1 1/2"	2"	2 1/2" - 3"	4"	5"	6"	8" - 10"	12" - 16"	18" - 24"	
$\lambda_T$	.027	.025	.023	.022	.021	.019	.018	.017	.016	.015	.014	0.013	0.012	
<b>MITRE BENDS</b>														
							$\alpha$ , degree	0	15	30	45	60	75	90
							N	2	4	8	15	25	40	60
<b>90° PIPE BENDS</b>														
							$r_c/D$	1	1.5	2	3	4	6	
							N	20	14	12	12	14	17	
							$r_c/D$	8	10	12	14	16	20	
							N	24	30	34	38	42	50	
<b>STANDARD BENDS</b>														
45 Standard Elbow							N = 16							
90 Standard Elbow							N = 30							
180 Close Pattern Return Bend							N = 50							
<b>CONTRACTIONS</b>														
							$K_2 = \frac{0.8(1-\beta^2)}{\beta^4} \sin \frac{\theta}{2}$	for $\theta \leq 45^\circ$						
							$K_2 = \frac{0.5(1-\beta^2)}{\beta^4} \sin \frac{1/2 \theta}{2}$	for $45^\circ < \theta \leq 180^\circ$						
<b>PIPE ENTRANCE</b>														
							$r/D$	0.00	0.02	0.04	0.06	0.10	0.15 & up	
							K	0.5	0.28	0.24	0.15	0.09	0.04	
<b>EXPANSIONS</b>														
							$K_2 = \frac{2.6(1-\beta^2)^2}{\beta^4} \sin \frac{\theta}{2}$	for $\theta \leq 45^\circ$						
Pipe Exit: $D \rightarrow \infty$							$K_1 = 1.0$							
							$K_2 = \frac{(1-\beta^2)^2}{\beta^4}$	for $45^\circ < \theta \leq 180^\circ$						
<b>VALVES</b>														
Gate Valve: $K = 8 \lambda_T$							Globe Valve: $K = 340 \lambda_T$							
K values are associated with the diameter in which the term $(v^2/2 g_c)$ occurs. The values in Table 2 are based on the following:														
ANSI Class	Class 300 and lower	Class 400 and 600	Class 900	Class 1500	Class 2500 (size 1/2" to 6")	Class 2500 (size 8" and up)								
PIPE SCHEDULE	40	80	120	160	XXS	160								

1.4. Flow through long bends and coils—fully-developed flows

Analytic treatments of flow through bends are easier when the flow is assumed to be fully-developed, which presumes the bend to be continuous, long and gradual. The classical treatment of the slow, fully-developed, laminar Newtonian flow in a curved pipe is due to Dean (1927, 1928). Various extensions of the approximation due to Dean have been carried out by van Dyke (1978), Barua (1963), Mori and Nakayama (1965) and Ito (1969). Further results include the

numerical solution of Collins and Dennis (1975), experimental data by White (1929), Adler (1934), Keulegan and Beij (1937) and Ito (1959), and the empirical correlation of White (1929). These are all concerned with laminar flow. Relationships for delineating laminar–turbulent transition in curved tube flow have been proposed by Ito (1959) and Ward-Smith (1980). For fully-developed turbulent flow Ito (1959) developed the empirical correlation

$$f_c(D/2r_c)^{1/2} = 0.00725 + 0.076[\text{Re}(D/2r_c)^2]^{-0.25} \quad [11]$$

which is good for  $0.034 < \text{Re}(D/2r_c)^2 < 300$ . In [11]  $D$  is the tube diameter,  $f_c$  is the curved-tube friction factor, and  $r_c$  is the radius of curvature of the bend. For  $(D/2r_c)^2 < 0.034$  the friction factor for the curved pipe is virtually identical to that for a straight pipe.

### 1.5. Flow through bends with long tangents

Short circular-arc bends connected to long straight upstream and downstream tangents are of greater practical interest. But here while the flow in the tangent lines can be fully-developed, that within the bend is developing. As a result the analysis of the flow is much more difficult. Of course, practically, turbulent flow is of most interest. Pressure losses and friction factors for turbulent Newtonian flow in curved pipes have been determined by Ito (1959, 1960). Using an extensive body of data on the flow of water through  $45^\circ$ ,  $90^\circ$  and  $180^\circ$  bends, Ito (1960) has presented plots in the form of  $K/\Theta(2r_c/D)^{1/2}$  vs  $\text{Re}(D/2r_c)^2$ , in which  $\Theta$  is the deflection angle of the bend in radians, and  $K$  is the friction loss or resistance coefficient defined in terms of the total head loss  $h_t$  attributable to the bend. The head loss is given by

$$K = h_t/(V^2/2) = (h_c + h_d + h_L)/(V^2/2). \quad [12]$$

The total head loss in the bend is assumed to be comprised of three components: (1) the loss due to curvature,  $h_c$ ; (2) the excess loss in the downstream tangent of the bend,  $h_d$ ; and (3) the loss due to the physical length of the bend. Since the physical length of the bend is  $L = r_c\Theta$ , the resistance coefficient,  $K_{\text{excl.}}$ , excluding the contribution due to  $h_L$ , is given by

$$K_{\text{excl.}} = K - 4f\Theta(r_c/D) \quad [13]$$

in which  $f$  is the usual friction factor for flow in a straight pipe.

Ito (1960) further provides the following empirical correlations based on the entire collection of data:

$$K = 0.03492\alpha f_c \theta (2r_c/D) \quad \text{for } \text{Re}(D/2r_c)^2 < 91 \quad [14]$$

$$K = 0.00241\alpha \theta \text{Re}^{-0.17} (2r_c/D)^{0.84} \quad \text{for } \text{Re}(D/2r_c)^2 > 91 \quad [15]$$

in which  $\theta$  is the deflection angle of the bend in degrees, i.e.  $\theta = (180/\pi)\Theta$ ,  $f_c$  is the friction factor for curved-tube flow given by [11], and  $\alpha$  depends on the relative radius as follows:

$$\theta = 45^\circ: \quad \alpha = 1.0 + 14.2(2r_c/D)^{-1.47} \quad [16a]$$

$$\theta = 90^\circ: \quad \alpha = 0.95 + 17.2(2r_c/D)^{-1.96} \quad \text{for } (2r_c/D) < 19.7 \quad [16b]$$

$$\theta = 90^\circ: \quad \alpha = 1.0 \quad \text{for } (2r_c/D) > 19.7 \quad [16c]$$

$$\theta = 180^\circ: \quad \alpha = 1.0 + 116(2r_c/D)^{-4.52}. \quad [16d]$$

### 1.6. Flows with changes in cross-section and shape of flow passage

The flow path through contractions, expansions and the Venturi meter involve changes in cross-sectional area. The flow through valves usually involves a combination of changes in flow path, including cross-section, shape and direction. Friction losses for flow through valves are expressed in terms of the resistance coefficient,  $K$ , defined by [8]. We employed only two types of valves in this study; the gate and globe valves. These, however, represent the limits of low and high resistances, respectively, and are the bases of most valve designs.

Losses associated with the laminar flow of non-Newtonian fluids through sudden contractions

and enlargements are important in capillary rheometry (Boger *et al.* 1978; Macagno and Hung 1967; Halmos *et al.* 1975). For fully turbulent Newtonian flow through a sudden expansion the friction loss is given by (Bird *et al.* 1960)

$$K_{\text{expn.}} = h_f/[V_1^2/2] = (1 - \beta^2)^2 \quad [17]$$

where  $\beta = (D_1/D_2) < 1$  is the ratio of upstream to downstream pipe diameters, and  $V_1$  is the velocity in the smaller (upstream) pipe. For turbulent flow in a sudden contraction, the friction loss is given by (Turian *et al.* 1983)

$$K_{\text{contr.}} = h_f/[V_2^2/2] = 0.45(1 - \beta^2)^2 \quad [18]$$

in which now  $\beta = (D_2/D_1) < 1$  is the ratio of downstream to upstream pipe diameters, and  $V_2$  is the velocity in the smaller (downstream) pipe.

To correlate the resistance coefficients for various fittings over the entire range of Reynolds numbers, Hooper (1981) proposed the use of two limiting values of coefficients  $K_1$  and  $K_\infty$  such that

$$K = (K_1/\text{Re}) + K_\infty. \quad [19]$$

Thus  $K_1 \sim K$  for  $\text{Re} = 1$ , since  $K_\infty \ll K_1$ , and  $K = K_\infty$  as  $\text{Re} \rightarrow \infty$ . Clearly, this does not signify that [19] is valid to  $\text{Re}$  values as low as 1. Indeed, this form is only applicable to large Reynolds numbers. A listing of values of  $K_1$  and  $K_\infty$  for various fittings is given by Hooper (1981).

Application of the macroscopic balances for flow through a Venturi meter with a throat diameter  $D_2$  in a pipe of diameter  $D_1$  gives for the mass rate of flow,  $w$

$$w = \rho \left( \frac{\pi}{4} D_1^2 \right) V_1 = C_v A_2 \left[ \frac{2(P_1 - P_2)\rho}{1 - \beta^4} \right]^{1/2} \quad [20]$$

in which  $\beta = (D_2/D_1) < 1$  is the ratio of the throat to pipe diameter,  $A_2 = (\pi D_2^2/4)$ . The parameter  $C_v$  is the discharge coefficient which, as the ratio of the mass flow rate in the actual flow to that in the ideal situation, accounts for the friction losses and the fact that velocity profiles across the sections 1 and 2 may not be flat. The loss in a Venturi meter is usually small, and  $C_v \sim 0.95-0.98$ . An analysis of the incompressible fluid flow through a Venturi meter using the macroscopic balances gives

$$C_v = \left[ \frac{1 - \beta^4}{\alpha_2 - \alpha_2 \beta^4 + \left( \Delta P_{\text{loss}} / \frac{1}{2} \rho V_2^2 \right)} \right]^{1/2} \quad [21]$$

in which  $\alpha = \overline{u^3}/\bar{u}^3$  is the kinetic energy correction factor and  $\Delta P_{\text{loss}} = \rho h_f$  is the irreversible loss of pressure due to friction. A summary of investigations of the flow through Venturi and differential-pressure flowmeters has been presented by Benedict (1977, 1980). Boundary-layer analyses for laminar and turbulent flow in a Venturi give the following relations:

$$C_v = \left[ \frac{1 - \beta^4}{1 - \beta^2 + 9.7158\beta^{1/2}\text{Re}^{-1/2} - 0.4505\beta^4\text{Re}^{-1/5}} \right]^{1/2} \quad \text{for } \text{Re}_t < 1 \times 10^5 \quad [22]$$

$$C_v = \left[ \frac{1 - \beta^4}{1 - \beta^4 + (0.17\beta^{1/5} - 0.4505\beta^4)\text{Re}^{-1/5}} \right]^{1/2} \quad \text{for } \text{Re}_t > 1 \times 10^5 \quad [23]$$

in which  $\text{Re} = \text{Re}_1$  and  $\text{Re}_t = \text{Re}_2$  are Reynolds numbers based on velocities and diameters in the pipe (inlet) and throat sections, respectively;  $\text{Re} = \beta \text{Re}_t$ .

### 1.7. Flow of non-Newtonian fluids and suspensions through complex geometries

Non-Newtonian flow through complex geometries is clearly of practical interest owing to the industrial importance of polymer processing operations. Studies on friction losses for the flow of non-Newtonian fluids and/or suspensions through bends, fittings, valves and flow meters are scarce. Some studies on the laminar flow of non-Newtonian, including viscoelastic, fluids through contractions have been carried out (Boger *et al.* 1978). These were motivated by the needs of rheometry. Among the few studies involving turbulent flow are those by Harris and Magnall (1972) on the flow of aqueous solutions of carboxymethyl cellulose and polyacrylamide in a 5.0 cm pipeline containing several sizes of orifice meters and one Venturi meter. Their attempt to correlate discharge coefficients using the Metzner and Reed generalized Reynolds number was evidently not successful. However, plots of  $\log \Delta P$  vs  $\log V$  resulted in parallel straight lines for the different orifice to pipe diameter ratios. No analogous trends could be established for the Venturi meter because data for only one device were available. Brook (1962) used the Venturi, the orifice, the 90° bend and the vertical counterflow meters to measure velocities and concentrations of suspensions. His conclusion was that the Venturi meter was the most accurate device of the four for use with suspensions, and that the best installed position was vertical. Shook and Masliyah (1974) studied the effect of slip associated with large and dense suspended particles on the discharge coefficient of the Venturi meter, and found that under such conditions the coefficient could be larger than one. For suspensions of fine particles the discharge coefficient can be predicted using the same equations as for the single phase fluid provided the suspension density is used (Brook 1962; Herringe 1977; Hanson *et al.* 1982). This is, of course, only true in turbulent flow. Mukhtar *et al.* (1995) report pressure drops for flow of water and of slurries of iron ore slimes and zinc tailings through a single 90° long radius bend. The measurements are made just across the bend, and no attempt seems to have been made to measure pressure losses along connecting tangent lines, although a long upstream tangent line is reported to have been provided. In a much more extensive investigation, Turian *et al.* (1983) considered the flow of settling noncolloidal suspensions of coarse, dense particles in water through an array of 2.5 and 5.0 cm bends, fittings, and valves. They found that friction losses for turbulent slurry flow could be predicted from the asymptotic values for single-phase flows provided the slurry density is used.

## 2. FRICTION LOSSES FOR FLOW OF SLURRIES THROUGH PIPING ELEMENTS

Experiments on the flow of the laterite and gypsum slurries through 2.5 and 5.0 cm bends, fittings, valves and Venturi meters were carried out. The array of piping elements used in this study

Table 2. Bends, fittings, valves and flowmeters used in slurry flow experiments

2.5 cm pipe: $D = 2.664$ cm	5.0 cm pipe: $D = 5.250$ cm
<i>Bends</i>	<i>Bends</i>
45° elbow, standard	45° elbow, standard
90° elbow, mitre ( $r_c = 0$ )†	90° elbow, mitre ( $r_c = 0$ )
90° elbow, standard ( $r_c = 3.8$ cm)	90° elbow, standard ( $r_c = 5.7$ cm)
90° elbow, smooth ( $r_c = 11.4$ cm)	90° elbow, smooth ( $r_c = 22.9$ cm)
90° elbow, smooth ( $r_c = 21.6$ cm)	90° elbow, smooth ( $r_c = 43.2$ cm)
90° elbow, smooth ( $r_c = 31.8$ cm)	90° elbow, smooth ( $r_c = 63.5$ cm)
180° open-pattern return bend	180° open-pattern return bend
<i>Valves</i>	<i>Valves</i>
Gate valve	Gate valve
Glove valve	Glove valve
<i>Venturi meters</i>	<i>Venturi meters</i>
$\beta = 0.5$ and $\beta = 0.75$ ‡	$\beta = 0.5$ and $\beta = 0.75$
<i>Fittings</i>	
$2.5 \times 5.0$ cm <sup>2</sup> sudden enlargement	
$2.5 \times 5.0$ cm <sup>2</sup> sudden contraction	

† $r_c$  is the radius of curvature of the bend.

‡ $\beta$  is the ratio of throat to pipe diameter.



Table 3. Mean resistance coefficients for turbulent flow of water in 2.5 cm fittings

Fitting	$\bar{K}_{(T)} = \bar{K}_{\infty} \dagger$	$ \%Dev.  \ddagger$	No. data	Table 1
45° elbow, standard	$0.81 \pm 0.132$	6.1	60	0.37
90° elbow ( $r_c = 0$ )	$1.66 \pm 0.158$	3.8	57	1.38
90° elbow ( $r_c = 3.8$ cm)	$1.11 \pm 0.163$	6.1	55	0.69
90° elbow ( $r_c = 11.4$ cm)	$0.77 \pm 0.083$	4.2	17	0.34
90° elbow ( $r_c = 21.6$ cm)	$0.95 \pm 0.123$	5.1	44	0.59
90° elbow ( $r_c = 31.8$ cm)	$1.21 \pm 0.175$	5.9	14	0.81
180° return	$1.07 \pm 0.104$	3.9	43	1.15
Gate valve	$0.80 \pm 0.120$	6.2	36	0.18
Globe valve	$10.0 \pm 0.750$	3.0	58	7.82

$\dagger \bar{K}_{(T)} = \bar{K}_{\infty} = \pm 2\sigma$ , signifying 95% confidence limit.

$\ddagger |\%Dev.|$  = average absolute per cent deviation from mean.

is listed in table 2. These piping elements were incorporated within several 2.5 and 5.0 cm test flow loops in our slurry pipeline facility. A detailed description and diagrams of this pilot facility are given by Ma (1987). In our experimental design each piping element was installed between long upstream and downstream developing sections, referred to as tangent lines, which consisted of straight pipe sections of the same diameter as the element. The axial pressure distributions along upstream and downstream tangents were measured using multitube differential mercury manometers. Flow loops containing long straight-pipe test sections, consisting of 1.25, 2.5 and 5.0 cm diameter galvanized as well as black steel pipe, were also part of the slurry flow facility, as described in our earlier paper on flow through straight pipe. They were used to measure straight-pipe flow pressure drops for each slurry flow rate through each of the fittings (see Turian *et al.* 1997).

### 2.1. Resistance coefficients including and excluding contribution due to fitting length— $K$ and $K_{excl.}$

Experimental determination of the resistances for fittings and valves is ordinarily carried out by measuring the overall friction loss for a system made up of two or more lengths of straight pipes connected in series by a number of fittings or valves of the same internal diameter. To obtain the loss due to the fitting or valve only, the losses in the straight pipes are subtracted from the overall friction loss. In this work the pressure drop between the upstream and farthest downstream pressure taps is taken as the overall pressure drop for the entire system containing the test fitting.

In pipeline design the overall length of straight pipe in the system may be calculated in one of two ways; depending upon whether or not the physical lengths of the bends, fittings and valves are included. If the physical lengths of these piping elements are included in the total length of straight pipe, then the friction losses, or resistance coefficients, for the individual flow elements must exclude a contribution corresponding to friction loss in a straight pipe of length equal to the physical length of the fittings. Referring to figure 1, this friction loss corresponds to the pressure drop given by  $C''C'$ . According to figure 1, the total distance, measured along the axis of the system from upstream to downstream pressure taps including the fitting, is  $L_m$ , and the total length of straight pipe is therefore  $(L_m - L_f)$ . Thus, we have

$$K = \frac{1}{\left(\frac{1}{2}\right)\rho V^2} \left[ -\Delta P_m - (L_m - L_f) \left( -\frac{\Delta P}{L} \right)_s \right] \quad [24]$$

and

$$K_{excl.} = \frac{1}{\left(\frac{1}{2}\right)\rho V^2} \left[ -\Delta P_m - L_m \left( -\frac{\Delta P}{L} \right)_s \right] \quad [25]$$

in which  $(-\Delta P/L)_s$  is the axial pressure gradient for fully-developed flow in the straight section of pipe containing the fitting. Detailed results on the flow of water and of the test slurries through

straight pipe are presented in the first part (Turian *et al.* 1997). In terms of the friction factor  $f$  for flow through straight pipe, the relationship between these resistance coefficients is given by

$$K = K_{\text{excl.}} + 4f(L_t/D). \quad [26]$$

2.2. Friction losses for flow of water through bends and fittings

Data on the flow of water through all the piping elements listed in table 2 were taken over the entire range of flow rates before and after each series of tests involving each test slurry. Our collection of baseline water data for each piping element is quite large, providing both a calibration for each fitting, and the basis for assessing inherent variability of measured resistance coefficients.

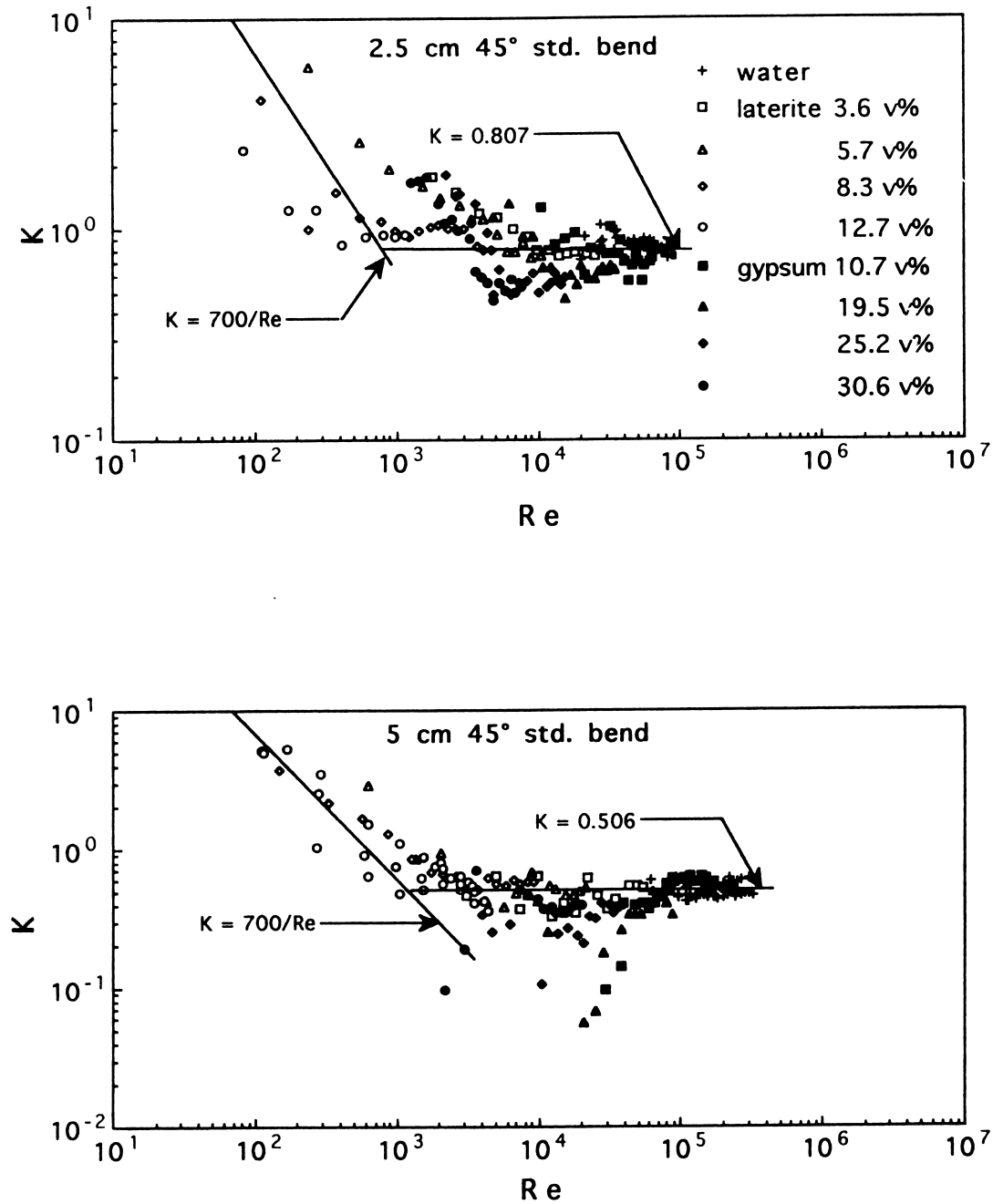


Figure 2. Resistance coefficients  $K$  vs  $Re_m$  for standard 45° elbows.

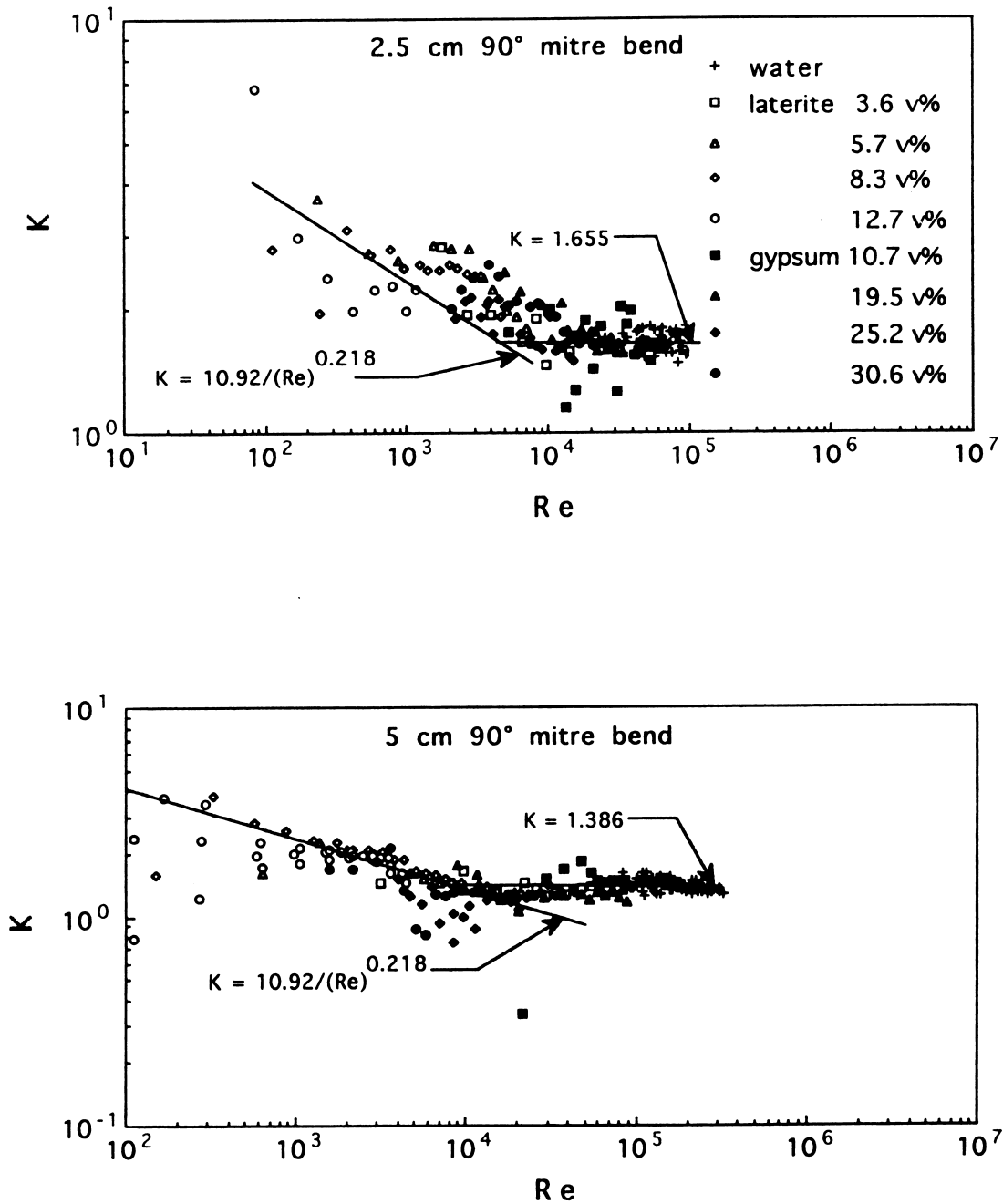


Figure 3. Resistance coefficients  $K$  vs  $Re_m$  for 90° mitre bends ( $r_c/D = 0$ ).

The mean resistance coefficients for flow of water through the 1 and 2 in bends and valves are given in tables 3 and 4. All water flow data were in the turbulent flow regime, with Reynolds numbers ranging from  $2 \times 10^4$  to  $3.3 \times 10^5$ .

The friction loss coefficients for different flow rates for flow of water for each piping element varied about the mean value. The per cent deviations from the mean values were approximately normally distributed about 0. The mean resistance coefficients,  $\bar{K}_{(T)}$ , for water in fully-developed turbulent flow through the 1 and 2 in test bends and valves, given in tables 3 and 4, include the loss due to the length of the fitting. The absolute average per cent deviation,  $|\%Dev.|$ , signifies the average of the absolute values of deviations from the mean, and

is given by

$$|\overline{\%Dev.}| = \text{average absolute \% dev.} = \frac{(\sum |K - \bar{K}|/\bar{K})}{N} \times 100. \quad [27]$$

The standard deviation is defined by

$$\sigma = \text{standard deviation} = \left[ \frac{(\sum (K - \bar{K})^2)}{N - 1} \right]^{1/2} \quad [28]$$

in which  $N$  is the total number of data points.

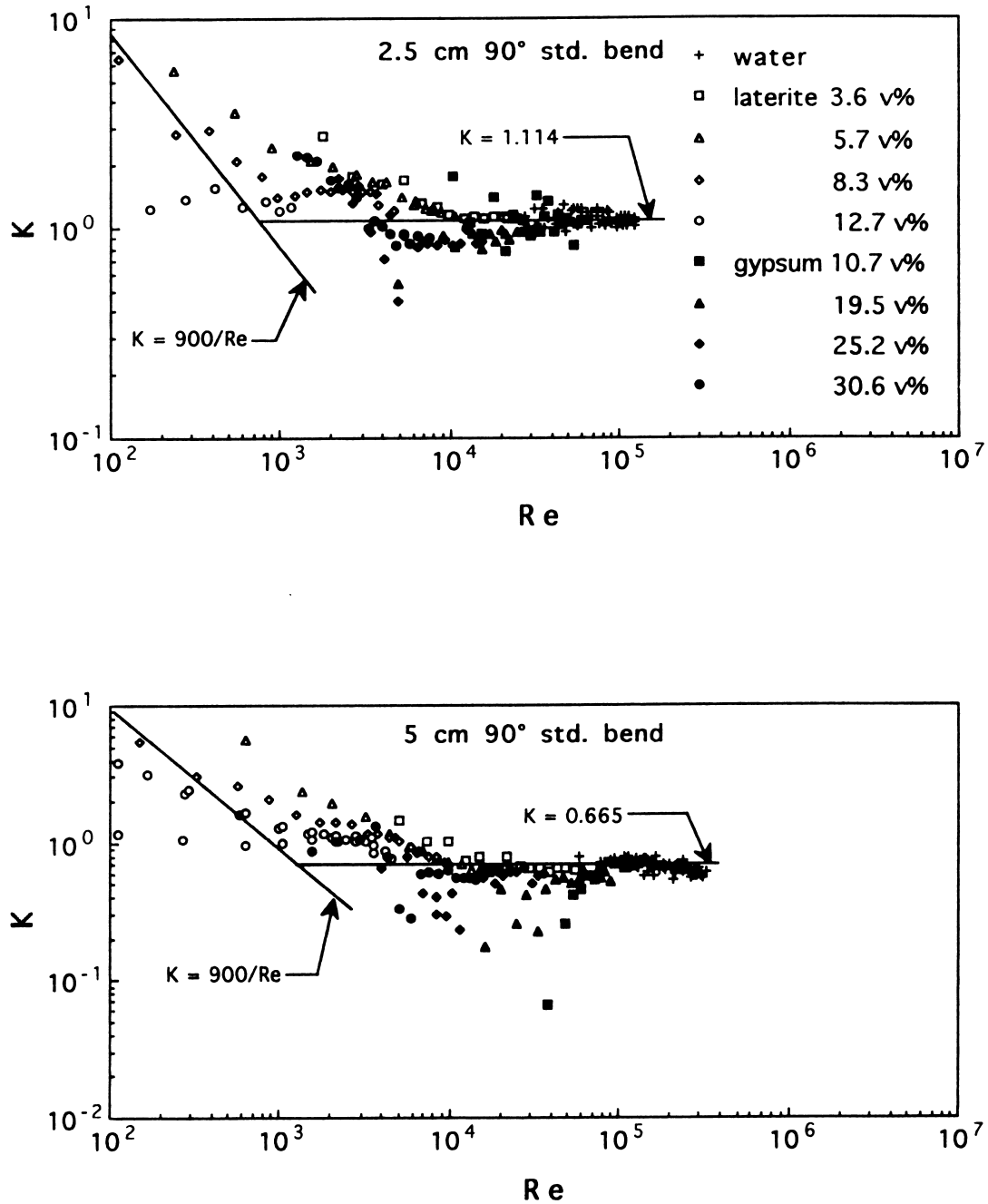


Figure 4. Resistance coefficients  $K$  vs  $Re_m$  for 90° standard bends ( $r_c/D = 2.25$ ).

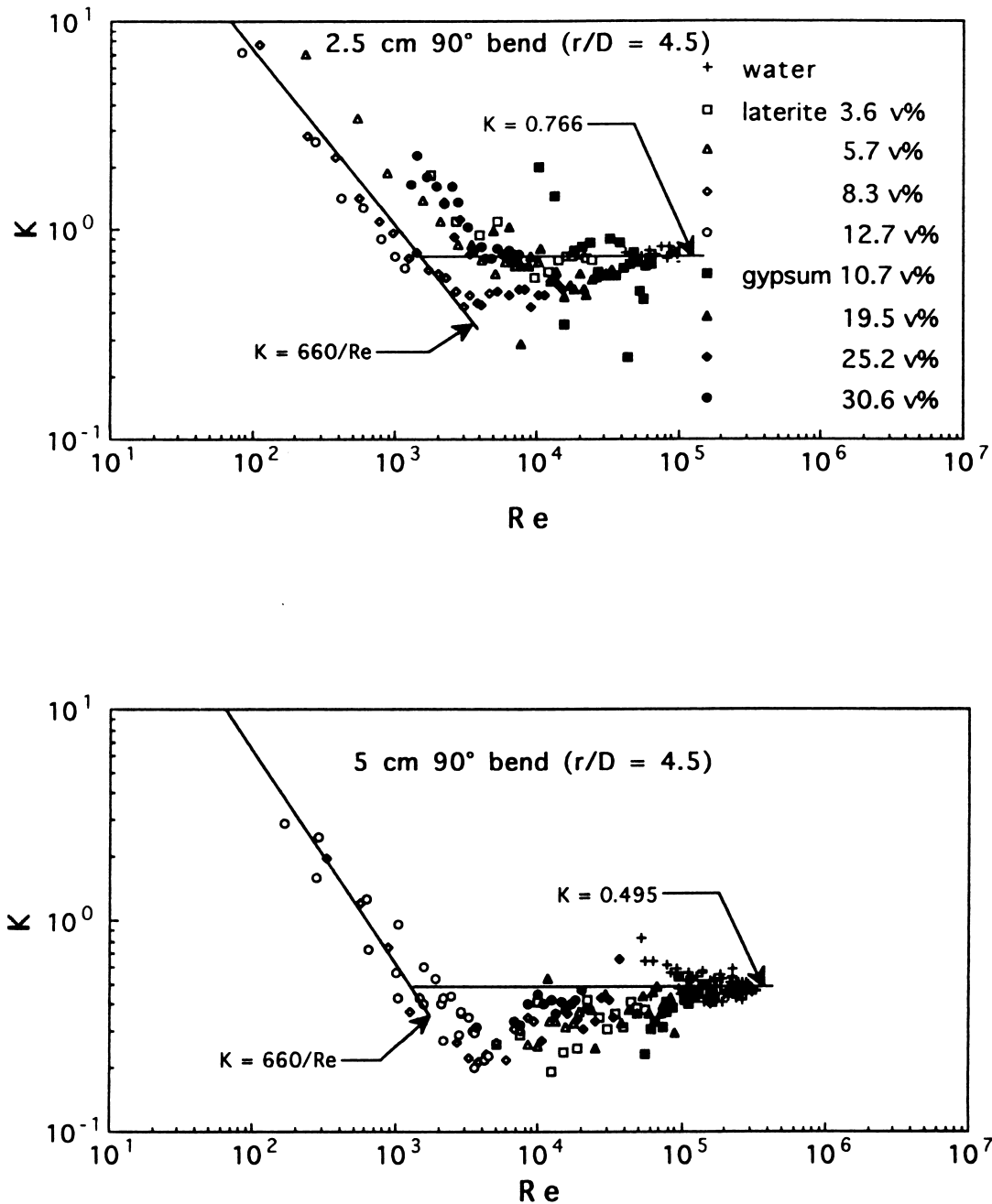


Figure 5. Resistance coefficients  $K$  vs  $Re_m$  for 90° bends ( $r_c/D = 4.5$ ).

For comparison we also include typical  $\bar{K}$  values from table 1, which are strictly applicable to turbulent flow. As stated before, these handbook values constitute typical approximate mean values that are merely representative. Strictly, they do not apply to our particular test fittings. Nonetheless, our measured mean resistance coefficients are in most cases quite close to the handbook values abstracted in table 1.

A further check on our results for water was to test them against Ito's (1960) correlations for turbulent flow through bends, given by [14]–[16]. The values of  $\bar{K}_\infty$  given in tables 3 and 4 are the means of large numbers of  $K$  vs  $Re$  data for the flow of water through each piping element. These primary  $K$  vs  $Re$  data, which will be presented in plots to be given later, are, therefore, appropriate for such a test. Ito's correlations were mainly found to underestimate our experimentally determined resistance coefficients; in some cases by up to a factor of two. It should be noted that

[14]–[16] were based on data taken using especially fabricated bends made of hydraulically smooth tubing stock. In our experiments we used standard 1 and 2 in (2.5 and 5.0 cm) off-the-shelf 45°, 90° and 180° commercial pipe elbows, and 90° pipe bends of different radii of curvature fabricated from commercial, straight steel piping stock. Our bends had surface roughness, which is not accounted for in Ito’s correlations.

The  $\bar{K}$  vs  $(r_c/D)$  results for the 90° bends seem to decrease to a minimum as  $(r_c/D)$  increases from the value 0 for the mitre bend, and then to increase with further increase in  $(r_c/D)$ . This is as expected. At first as  $(r_c/D)$  increases from the value 0 for the mitre bend, there is a net decrease in friction loss resulting from the fact that the change in direction of the flow is becoming gentler. This happens because the contribution to the total loss due to curvature,  $h_c$ , at first decreases more rapidly than the increase in the contribution due to the physical length of the fitting,  $h_L$  (see [12]).

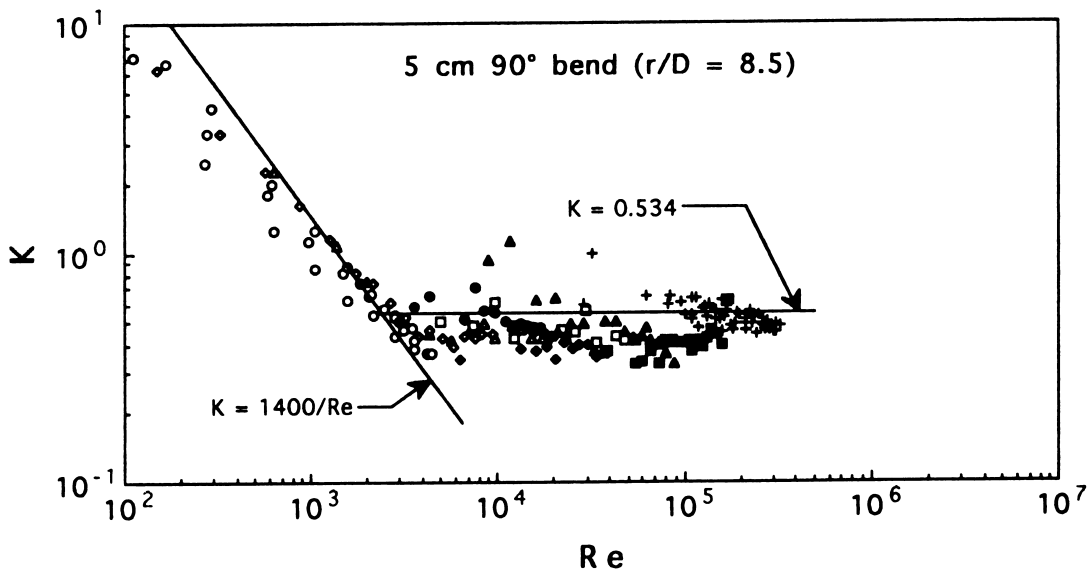
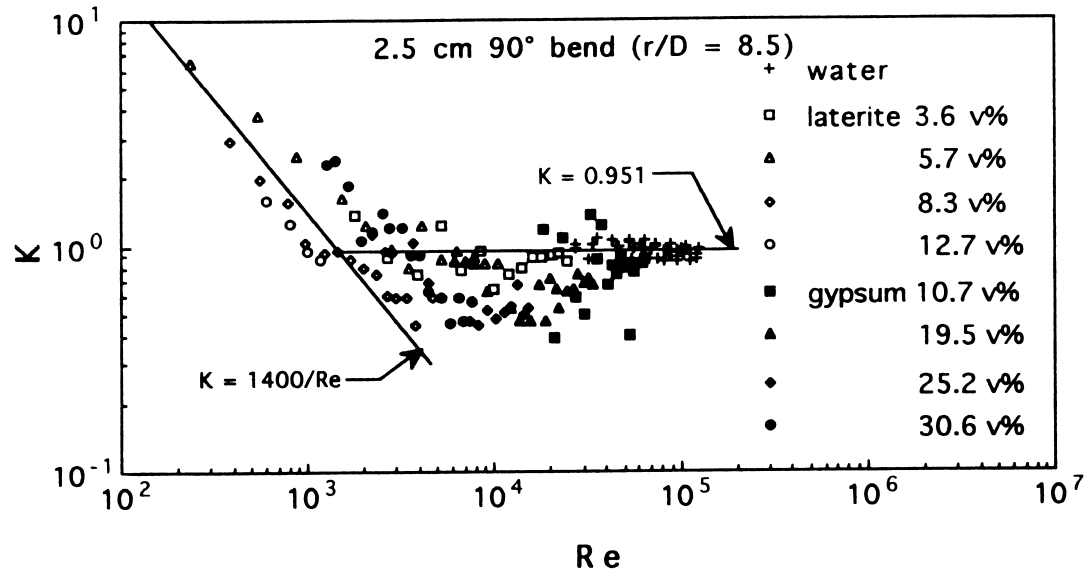


Figure 6. Resistance coefficients  $K$  vs  $Re_m$  for 90° bends ( $r_c/D = 8.5$ ).

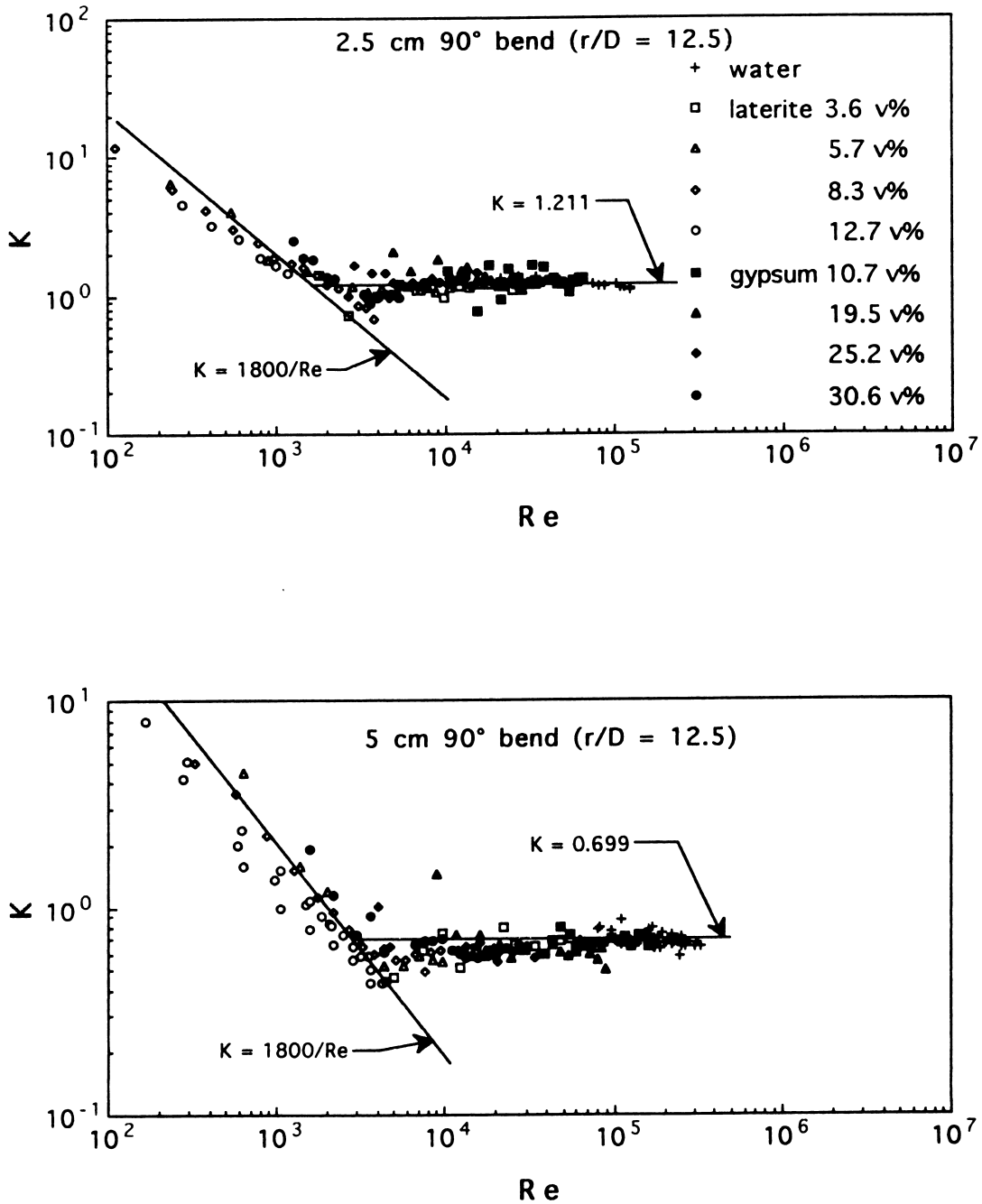


Figure 7. Resistance coefficients  $K$  vs  $Re_m$  for 90° bends ( $r_c/D = 12.5$ ).

Eventually, however, the rate of increase in the contribution due to increasing length of the fitting, as  $(r_c/D)$  increases further, exceeds the rate of decrease in the contribution due to curvature. The minimum in the  $\bar{K}$  vs,  $(r_c/D)$  dependence for our water data in tables 3 and 4 occurs at about  $(r_c/D) \sim 4.5$ , which is about the same value obtained with plots using the values from table 1.

A few important observations need to be noted in view of these water flow data. The absolute average per cent deviations of the resistance coefficients from the mean values ranged between about 3% and 15%, with the highest per cent deviations being associated with the piping elements having the lowest frictional losses, and/or at the lower flow velocities. Of course, this is partly because there is a limit to the level of attainable accuracy, in absolute terms, with such measurements. Furthermore, when the  $K$  vs  $Re$  data for each element are compared with the mean values, or are plotted as will be done below, it is found that the main body of the data falls mainly

within a 20% band around the mean value. This level of scatter in the measured values of  $K$  seems to be inherent to Newtonian flow through such complex geometries, since it is observed with replicated data, and since it seems not to be due to any discernible systematic variation with Reynolds number, except, of course, when there is a change in flow regime. The presence of a disturbance in the flow path may lead to increased turbulence, secondary flows, vortex formation and flow separation, depending upon the severity of the disturbance to the flow. The associated overall frictional losses may not be fully controllable inasmuch as the onset of some of these flow phenomena may be sensitive to subtle differences in experimental conditions (as well as the current condition of the device), and most likely so near transition conditions. The additional presence of suspended solids, and the appearance of non-Newtonian behavior, may reinforce these effects.

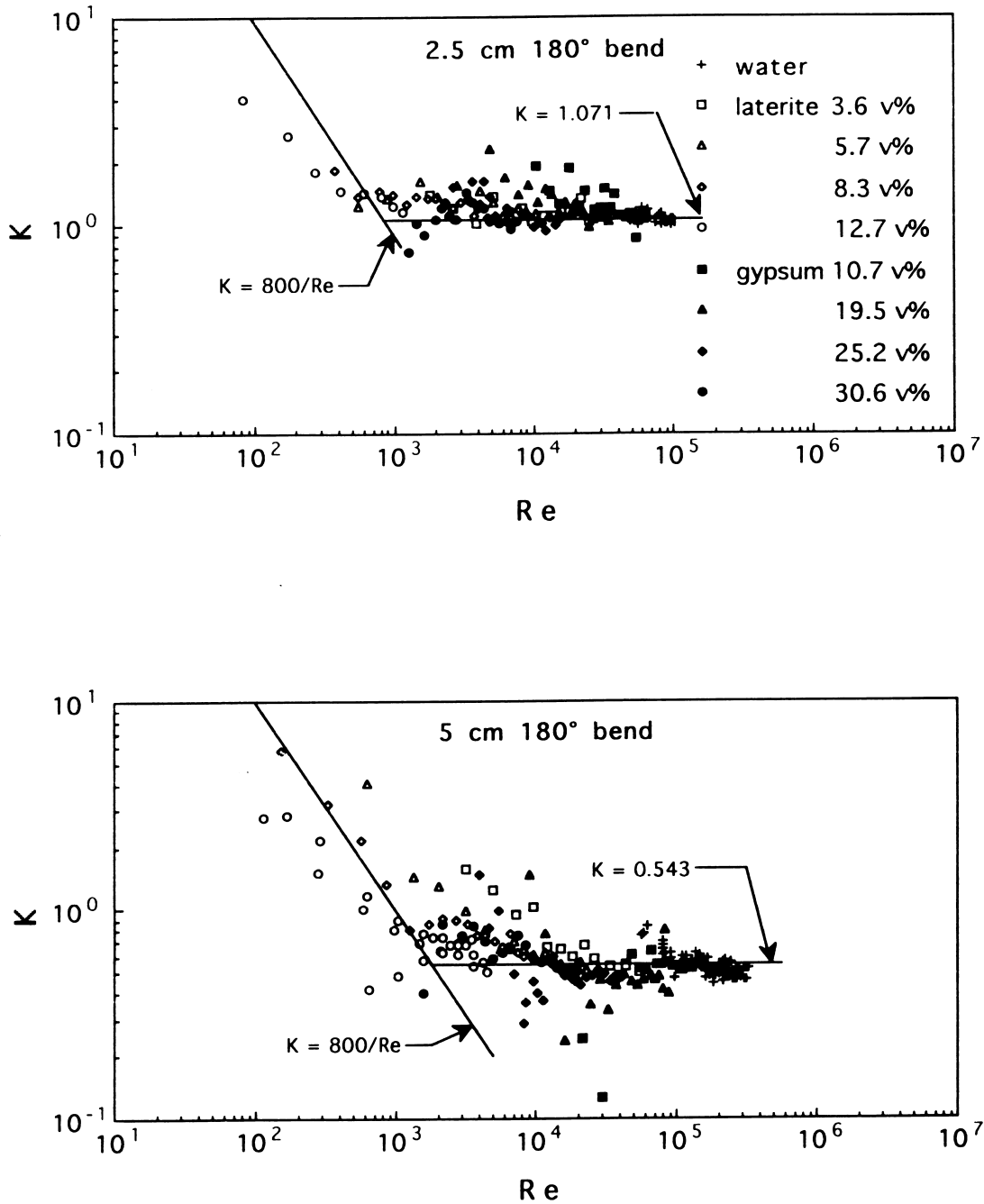


Figure 8. Resistance coefficients  $K$  vs  $Re_m$  for 180° open-pattern return bends.



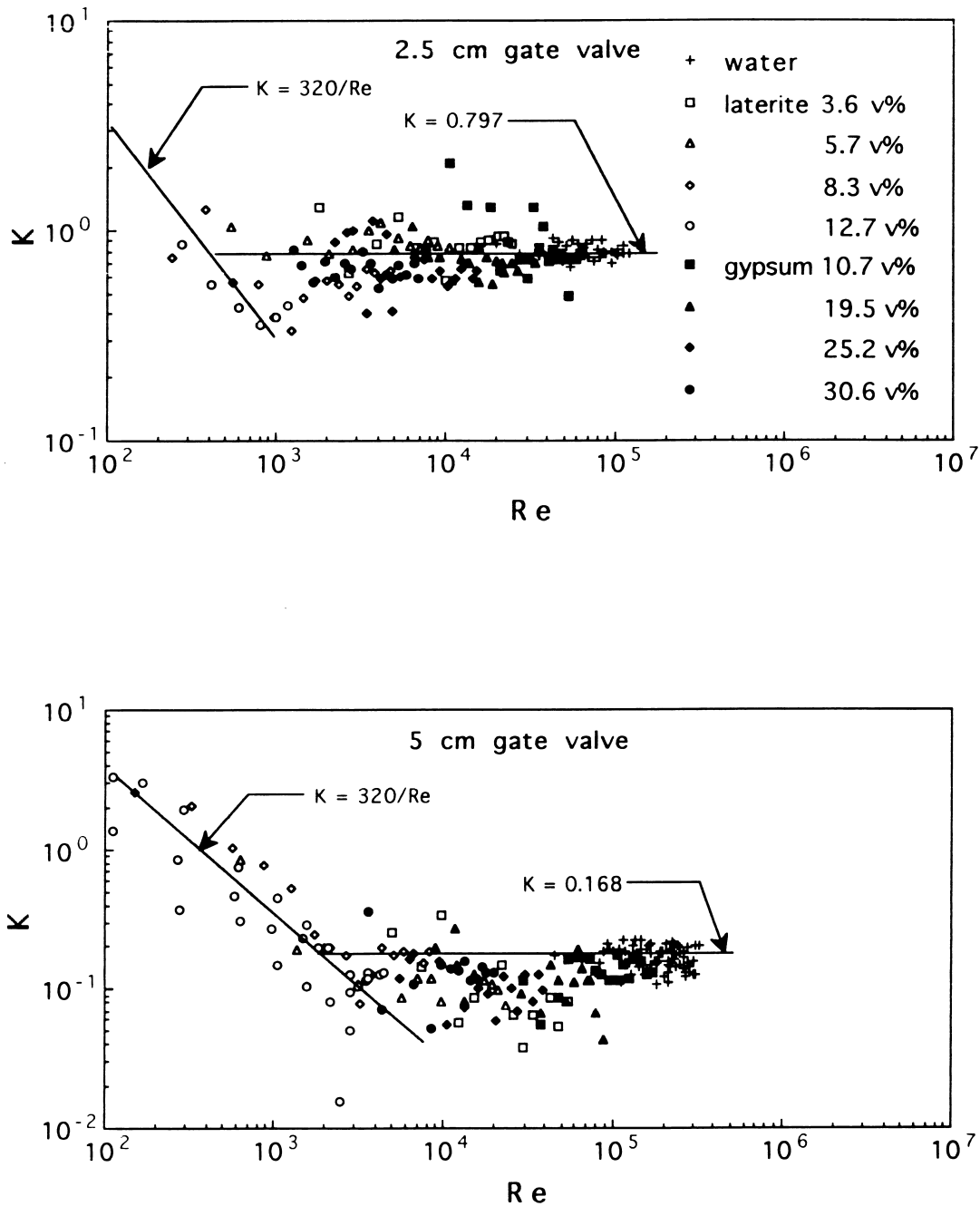


Figure 9. Resistance coefficients  $K$  vs  $Re_m$  for gate valves.

Accordingly, there seems to be an intrinsic limit to the level of reproducibility attainable in the measurement of resistance coefficients for such flows. These constraints will be useful as references against which our results for non-Newtonian suspension flow through complex geometries are assessed.

### 2.3. Flow of non-Newtonian slurries through bends and valves

We present first our results for the flow of the laterite and gypsum suspensions through the bends and valves. The results for the expansion, contraction and the Venturi meters will be presented afterwards. From the preceding discussion one would presume that the difference between the two values of the resistance coefficients, defined by [24]–[26], is that the coefficient  $K_{excl.}$  accounts strictly

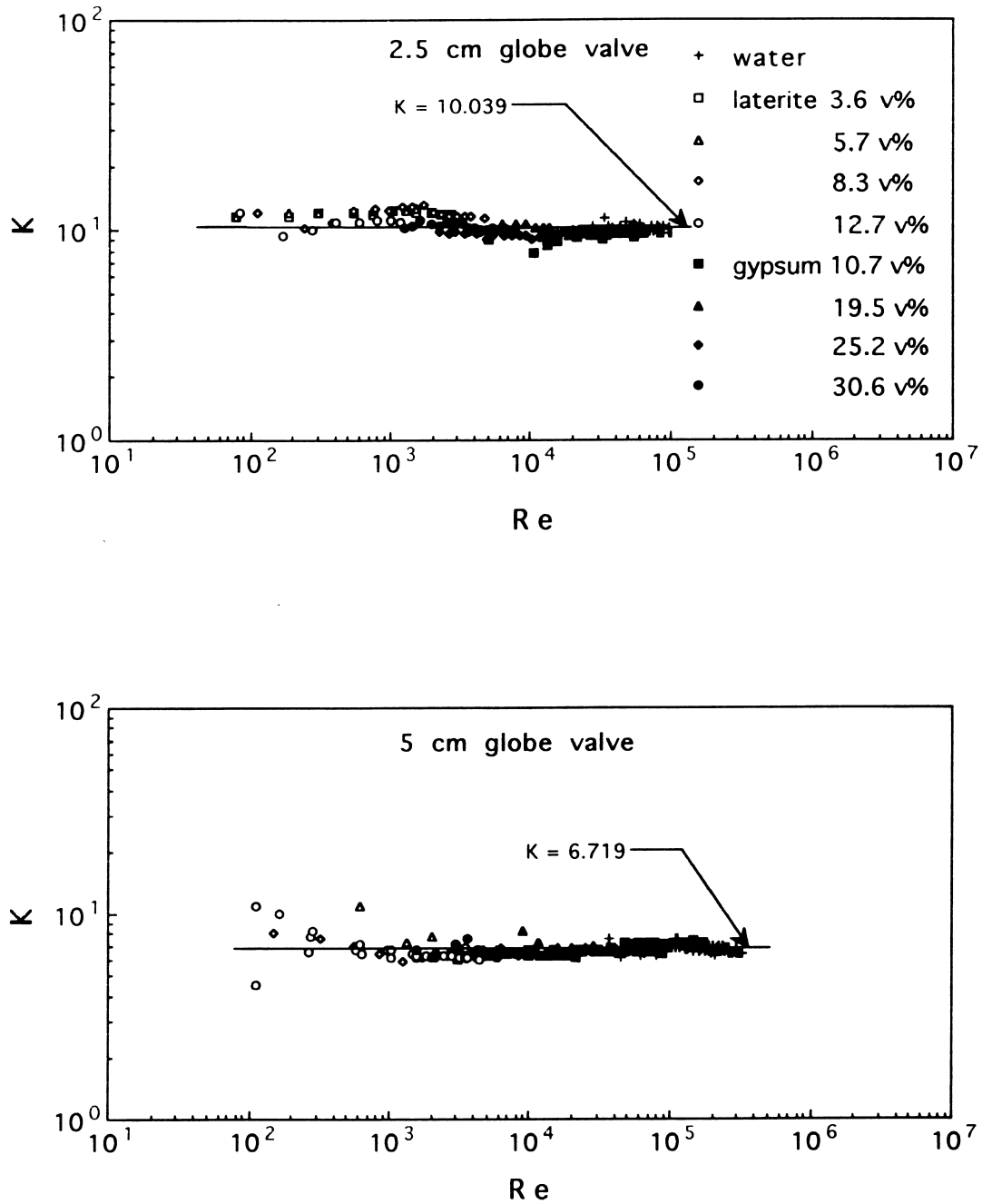


Figure 10. Resistance coefficients  $K$  vs  $Re_m$  for globe valves.

for only the additional loss (over that attributable to fully-developed flow through a straight pipe of the same physical length) arising from such flow disturbance-induced effects as increased turbulence, secondary flows, vortices or flow separation. We will, therefore, present results in terms of both  $K$  and  $K_{excl.}$  values.,

The experimental  $K$  values for each fitting were determined for different suspension flow velocities by measuring the axial pressure distributions along the fitting and its tangent lines. For each measurement, the temperature of the fluid and the pressure drop along a test section of straight pipe of the same diameter as the fitting were also determined. For each piping element the experimental  $K$  values were plotted, using logarithmic scales, against  $Re_m$  and also against  $Re_{\infty}$ .

Table 4. Mean resistance coefficients for turbulent flow of water in 5.0 cm fittings

Fitting	$\bar{K}_{(T)} = \bar{K}_{\infty} \dagger$	$ \%Dev.  \ddagger$	No. data	Table 1
45° elbow, standard	0.51 ± 0.110	9.2	51	0.30
90° elbow ( $r_c = 0$ )	1.39 ± 0.165	4.6	82	1.14
90° elbow ( $r_c = 5.7$ cm)	0.66 ± 0.129	7.7	78	0.57
90° elbow ( $r_c = 22.9$ cm)	0.50 ± 0.130	9.2	75	0.28
90° elbow ( $r_c = 43.2$ cm)	0.53 ± 0.168	10.2	56	0.48
90° elbow ( $r_c = 63.5$ cm)	0.70 ± 0.110	6.0	43	0.66
180° return	0.54 ± 0.144	9.5	80	0.95
Gate valve	0.17 ± 0.061	15.4	68	0.15
Globe valve	6.72 ± 0.584	3.4	85	6.46

† $\bar{K}_{(T)} = \bar{K}_{\infty} \pm 2\sigma$ , signifying 95% confidence limit.

‡ $|\%Dev.|$  = average absolute per cent deviation from mean.

Table 5. Comparison of predicted and measured  $K_{(L)}$  for laminar suspension flow through 2.5 and 5.0 cm fittings

Fitting	$\Phi$	$K_{(L)} = \Phi/Re_m$				$Re_m^*$	
		Range $Re_m \times 10^{-2}$	No. of data	Abs. av. % dev.†	No. in 0% band	2.5 cm	5.0 cm
45° elbow, standard	700	0.86–13.5	32	43.2	14	867	1383
90° elbow ( $r_c/D = 0$ )	—‡	—	—	—	—	—	—
90° elbow (standard)	900	0.82–12.6	30	60.0	12	807	1353
90° elbow ( $r_c/D = 4.5$ )	660	0.86–12.5	24	32.5	15	862	1333
90° elbow ( $r_c/D = 8.5$ )	1400	2.40–24.5	44	24.4	31	1472	2622
90° elbow ( $r_c/D = 12.5$ )	1800	1.14–24.5	47	21.1	36	1486	2575
180° return	800	0.86–14.7	26	41.2	14	747	1473
Gate valve	320	1.12–18.5	27	47.1	9	402	1905
Globe valve	—‡	—	—	—	—	—	—

†Absolute average of per cent deviation between predicted and measured  $K$ .

‡Data in laminar flow could not be obtained for these high-loss devices.

Table 6. Mean  $\bar{K}_{(T)}$  for turbulent suspension flow through 2.5 cm fittings

Fitting	$K_{(T)} = \bar{K}_{\infty}$	Range $Re_m \times 10^{-3}$	No. of data	Abs. av. % dev.†	No. of data in 30% dev. band.
45° elbow, standard	0.81	0.89–126	175	22.1	134
90° elbow ( $r_c = 0$ )	1.66	4.11–126	130	7.0	126
90° elbow ( $r_c = 3.8$ cm)	1.11	0.82–126	171	19.2	140
90° elbow ( $r_c = 11.4$ cm)	0.77	0.89–119	130	28.1	87
90° elbow ( $r_c = 21.6$ cm)	0.95	1.56–132	140	20.5	100
90° elbow ( $r_c = 31.8$ cm)	1.21	1.56–126	118	12.4	106
180° return	1.07	0.79–126	160	13.6	138
Gate valve	0.80	0.42–119	157	18.3	128
Globe valve	10.0	0.09–132	169	6.9	168

†Absolute average per cent deviation of  $K_{(T)}$  from mean  $\bar{K}_{\infty}$ .

Table 7. Mean  $\bar{K}_{(T)}$  for turbulent suspension flow through 5.0 cm fittings

Fitting	$K_{(T)} = \bar{K}_{\infty}$	Range $Re_m \times 10^{-3}$	No. of data	Abs. av. % dev.†	No. of data in 30% dev. band
45° elbow, standard	0.51	1.47–328	174	20.9	136
90° elbow ( $r_c = 0$ )	1.39	4.22–328	190	8.6	181
90° elbow ( $r_c = 5.7$ cm)	0.66	1.47–328	209	23.4	155
90° elbow ( $r_c = 22.9$ cm)	0.50	1.47–328	181	20.5	133
90° elbow ( $r_c = 43.2$ cm)	0.53	2.65–328	165	17.0	146
90° elbow ( $r_c = 63.5$ cm)	0.70	2.65–328	152	11.4	145
180° return	0.54	1.55–328	216	19.9	174
Gate valve	0.17	2.02–328	177	26.5	115
Globe valve	6.72	0.11–328	240	5.5	236

†Absolute average per cent deviation of  $K_{(T)}$  from mean  $\bar{K}_{\infty}$ .

Table 8. Resistance coefficients  $K_{\text{excl.}}$  for laminar and turbulent suspension flow through 2.5 and 5.0 cm fittings

Fitting	Laminar flow $K_{\text{excl. (L)}} = \Phi \text{Re}_m^{-\lambda}$		Turbulent flow $K_{\text{excl. (T)}} = \bar{K}_{\text{excl.}\infty}$	
	$\Phi$	$\lambda$	1 in	2 in
45° elbow, standard	150.5	0.701	0.76	0.50
90° elbow ( $r_c/D = 0$ )	12.88	0.242	1.62	1.33
90° elbow (standard)	36.81	0.441	1.04	0.62
90° elbow ( $r_c/D = 4.5$ )	76.40	0.678	0.63	0.39
90° elbow ( $r_c/D = 8.5$ )	310.4	0.884	0.70	0.30
90° elbow ( $r_c/D = 12.5$ )	61.64	0.665	0.84	0.40
180° return bend	90.77	0.629	1.00	0.48
Gate valve	1289.0	1.255	0.80	0.15
Globe valve†	—	—	10.0	6.65
2 × 1 in <sup>2</sup> contraction	142.4	0.763		0.230
1 × 2 in <sup>2</sup> expansion	115.1	1.000‡		0.5512

†Data in laminar flow could not be obtained for the high-loss devices.

‡For the expansion  $K_{\text{excl. (L)}} = 0.5512 + \Phi \text{Re}_m^{-1}$ .

$\text{Re}_m$  is the generalized Reynolds number given by

$$\text{Re}_m = D^{n'} V^{(2-n')} \rho / [8^{(n'-1)} K'] \quad [29]$$

in which  $n'$  is the local slope of the  $\log(D\Delta P/4L)$  vs  $\log(8V/D)$  curve for the suspension, and  $\text{Re}_\infty = DV\rho/\eta_\infty$  (see Turian *et al.* 1997).

The shapes of  $K$  vs  $\text{Re}$  curves, using  $\text{Re}_m$  or  $\text{Re}_\infty$ , turned out to be similar for each piping element; namely, the data points for the low- $\text{Re}$ , laminar-flow range seemed to be scattered about a straight line of slope  $-1$ , and those for the high- $\text{Re}$ , turbulent-flow regime seemed to define a horizontal line having the constant asymptotic value  $\bar{K}_\infty$ . Aside from this, there were three additional findings.

(1) when the data for the two sizes for each fitting were superimposed, the data in the laminar flow range overlapped, being scattered around the same straight line, on logarithmic scales, given by [30] below.

(2) For each fitting the turbulent-flow, horizontal-line asymptotes  $\bar{K}_\infty$  were different for the two sizes.

(3) The value of  $\bar{K}_\infty$  for each size of fitting turned out to be the same as the corresponding turbulent-flow resistance coefficient for the flow of water, given in tables 3 and 4.

The difference between the two types of plots, using the two different  $\text{Re}$  definitions, resides in the fact that the Reynolds number  $\text{Re}_\infty$  is perhaps less meaningful, since the viscosity parameter  $\eta_\infty$ , by itself, does not embody the full rheological characteristics of the fluid, and surely not in

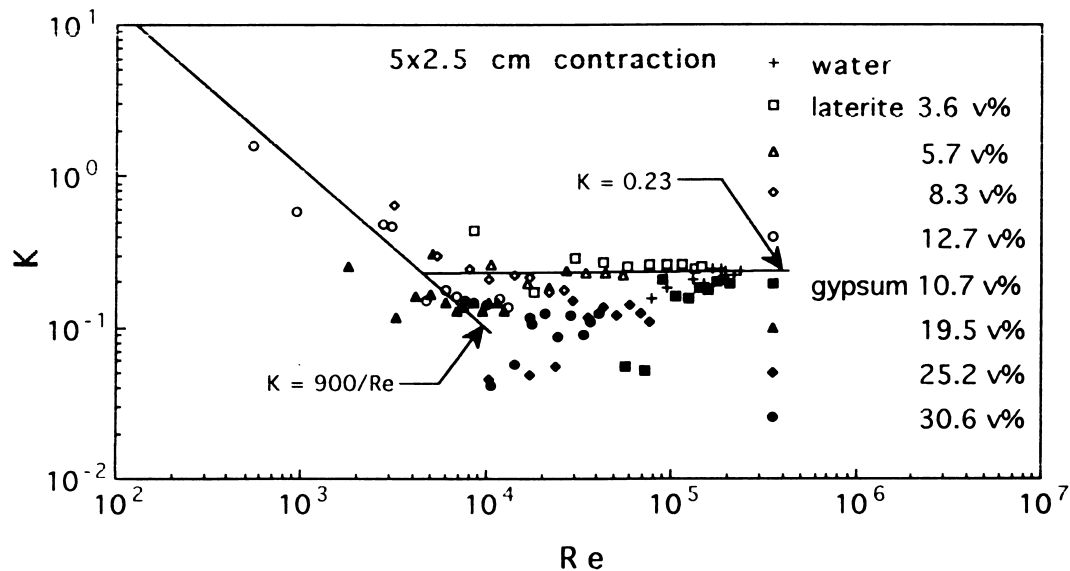


Figure 11. Resistance coefficient  $K_{\text{contr.}}$  vs  $\text{Re}_m$  for  $5.0 \times 2.5 \text{ cm}^2$  concentric contraction.

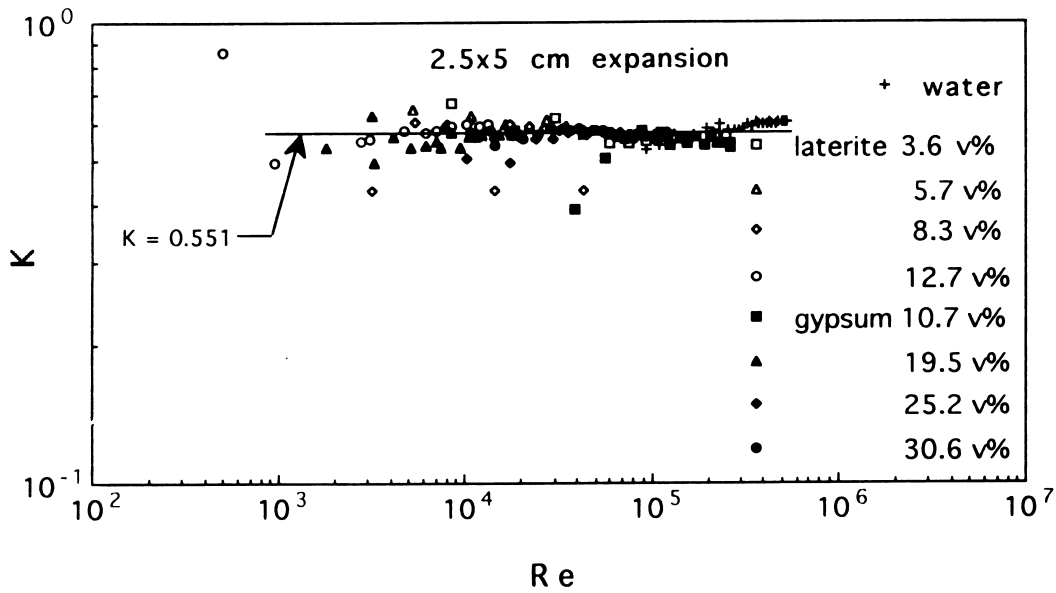
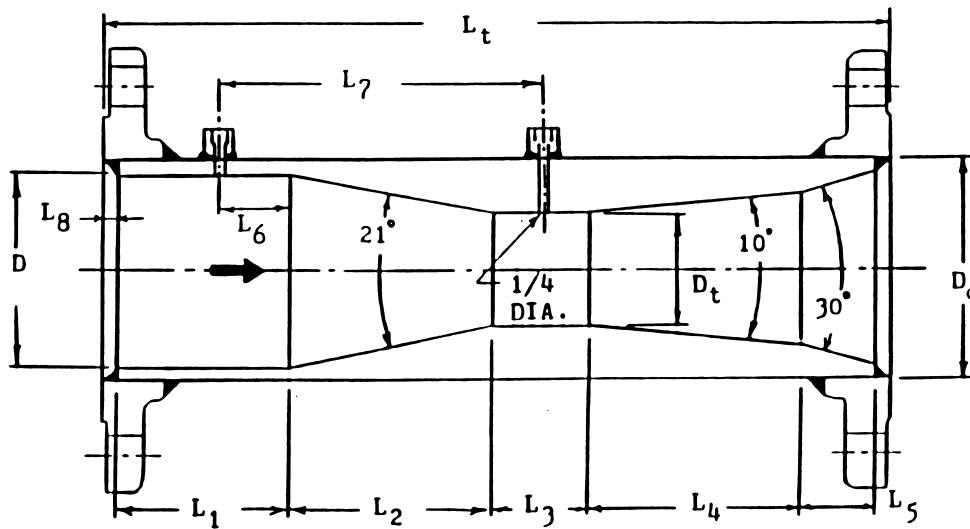


Figure 12. Resistance coefficient  $K_{expn.}$  vs  $Re_m$  for  $2.5 \times 5.0 \text{ cm}^2$  concentric expansion.

the laminar flow range. In the turbulent regime, since the asymptotic value of  $K$  is found to be constant in any event, the type of Reynolds number definition is irrelevant, except in delineating the point of laminar-turbulent transition for the particular type of piping element.

The friction loss data for water and suspension flow through our test bends and valves are given in figures 2 to 10 as plots of  $K$  against  $Re_m$ . For each type of fitting the data is presented in one figure, the two parts of which are designed to separate the plots for the two sizes, although the



Pipe	$\beta$	$D_0$	$D$	$D_t$	$L_1$	$L_2$	$L_3$	$L_4$	$L_5$	$L_6$	$L_7$	$L_8$	$L_t$
1"	0.75	1.315	1.049	0.787	2.84	0.71	1.00	1.05	0.15	1.00	2.21	0.12	6.00
1"	0.5	1.315	1.049	0.525	2.95	1.41	1.00	2.10	0.29	1.00	2.91	0.12	8.00
2"	0.75	2.375	2.067	1.550	2.75	1.39	1.20	2.07	0.29	1.00	2.99	0.15	8.00
2"	0.5	2.375	2.067	1.034	2.20	2.79	1.00	4.13	0.58	0.80	4.09	0.15	11.00

All dimensions are in inches.

Figure 13. Detailed diagram of Venturi meters.

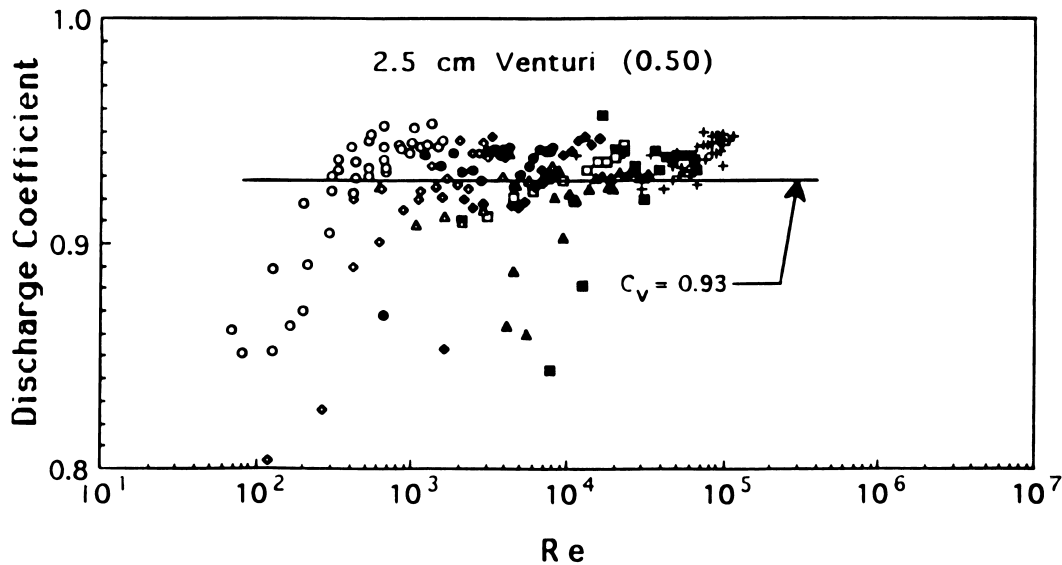
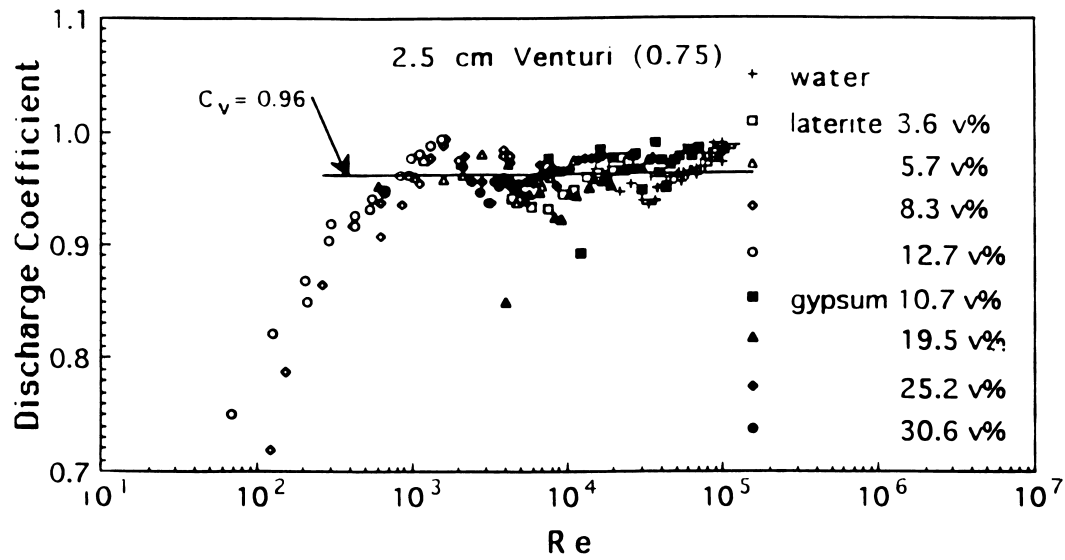


Figure 14. Discharge coefficients  $C_v$  vs  $Re_m$  for 2.5 cm<sup>2</sup> Venturi meters.

data in laminar flow do overlap. Figure 2 presents the data for the 45° standard bends, figures 3–7 present the data for the 90° bends of different radii of curvature, figure 8 presents the data for the 180° open-pattern return bend, and figures 9 and 10 present the data for the gate and globe valves, respectively.

The findings described in the foregoing lead to the following correlation for the resistance coefficients for laminar suspension flow through the 2.5 and 5.0 cm bends and valves:

$$K = K_{(L)} = A/Re_m \quad \text{for } Re_m \leq Re_m^* \quad [30]$$

The parameter  $A$  in the correlation [30] was found to have the same value for the two sizes of each type of bend or valve. The Reynolds number  $Re_m^*$  represents the laminar–turbulent transition value for the fitting, which turns out to be different for the two sizes of each type of fitting. The

values of  $A$  for the different test bends and valves, and of  $Re_m^*$  for the two sizes of fittings, are given in table 5.

The resistance coefficients for turbulent suspension flow,  $K_{(T)}$ , through the 1 and 2 in bends and valves are given in tables 6 and 7 as  $\bar{K}_\infty$ . These are the same as the mean resistance coefficients for turbulent flow of water designated as  $\bar{K}_\infty$  in tables 3 and 4. Accordingly, we have for turbulent non-Newtonian suspension flow through fittings the relation

$$K_{(T)} = \bar{K}_{(T)} = \bar{K}_\infty \quad \text{for } Re_m > Re_m^* \quad [31]$$

We also plotted the experimentally determined,  $K_{excl.}$ , defined by [25], for each fitting against the two Reynolds  $Re_m$  numbers and  $Re_\infty$  using logarithmic scales. As in the case of the  $K$  vs  $Re$  plots described in the foregoing, the data points in the laminar range were scattered about a straight

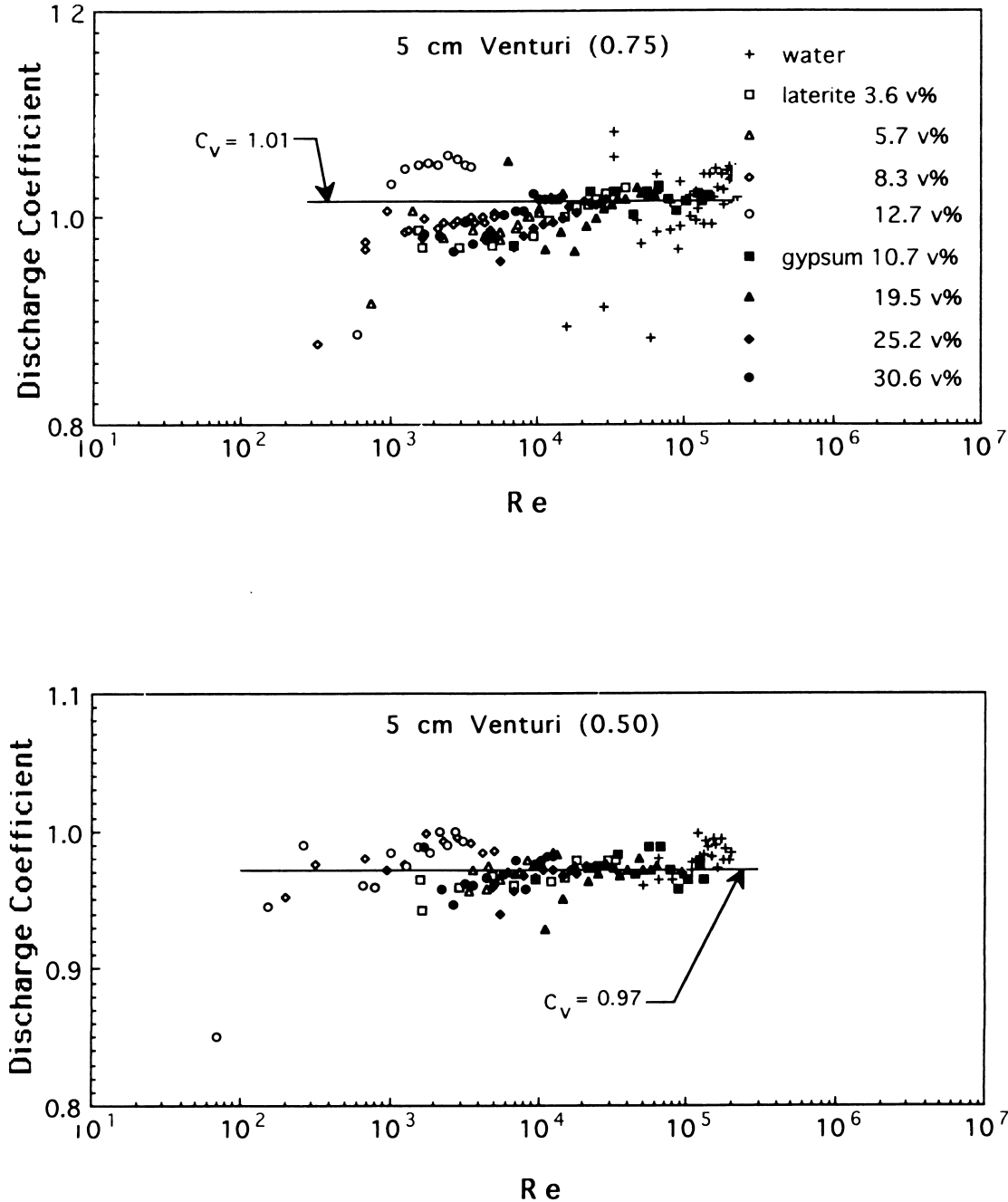


Figure 15. Discharge coefficients  $C_V$  vs  $Re_m$  for 5.0 cm<sup>2</sup> Venturi meters.

Table 9. Discharge coefficients,  $C_v$ , for water and suspension flow through 2.5 and 5.0 cm Venturi meters

Venturi meter	2.5 cm		5.0 cm	
$\beta = D_i/D$	0.50	0.75	0.50	0.75
$C_v$ range†	0.91–0.95	0.92–1.00	0.95–1.00	0.96–1.05
Average $\bar{C}_v$	0.93	0.96	0.97	1.01
$Re_m^*$	400	1000	700	1000

†Range of variation of  $C_v$  values about mean in turbulent flow;  $Re_m > Re_m^*$ .

line, which was the same for both sizes of fittings, but instead of having a slope of  $-1$ , as in [30], the slopes ( $= -\lambda$ ) were slightly larger for all fittings except the gate valve, i.e.  $0 < \lambda < 1$ . However, the  $K_{\text{excl.}}$  vs  $Re$  had more scatter than the  $K$  vs  $Re$  plots. This is due to the fact that the resistance coefficients  $K_{\text{excl.}}$ , being the differences between two quantities, which are for most of the fittings about the same magnitude, are subject to larger relative error. The equation for  $K_{\text{excl.}}$  ( $Re_m$ ) for laminar, non-Newtonian suspension flow through bends and fittings is given by

$$K_{\text{excl. (L)}} = \Phi Re_m^{-\lambda} \quad \text{for } Re_m \leq Re_m^* \quad [32]$$

where the constants  $\Phi$  and  $\lambda$ , which are the same for the two sizes of each type of fitting, are listed in table 8. The transition Reynolds numbers,  $Re_m^*$ , are the same as for [30], and are listed in table 5.

In turbulent flow it was found that the resistance coefficients,  $K_{\text{excl. (T)}}$ , for all bends and valves of the same size and type and all test fluids, water as well as suspensions, were scattered about the same horizontal asymptote, having the constant value given by

$$K_{\text{excl. (T)}} = \bar{K}_{\text{excl.}\infty} \quad \text{for } Re_m > Re_m^*. \quad [33]$$

Values of  $\bar{K}_{\text{excl.}\infty}$  are given in table 8. They are related to  $\bar{K}_{\infty}$  through [26].

#### 2.4. Flow of non-Newtonian slurries through expansions and contractions

As in all the preceding, in considering flows through contractions and expansions we designate the upstream section by numeral 1 and the downstream by 2. Resistance coefficients for both expansion and contraction are defined in terms of the velocity in the smaller cross-section.

Applying the macroscopic mechanical energy balance [1] to flow through a contraction, we get

$$K_{\text{contr.}} = [h_f/(V_2^2/2)] = [-\Delta P/(\rho V_2^2/2)] + (\beta^4 - 1) \quad [34]$$

in which  $\beta = (D_2/D_1) < 1$ . For our  $2.5 \times 5.0 \text{ cm}^2$  ( $2 \times 1 \text{ in}^2$  standard pipe) concentric contraction,  $\beta = (1.049/2.067) = 0.5075$ . For turbulent Newtonian flow through a sudden contraction a rough estimate that is used is  $K_{\text{contr.}} \sim 0.5$ , while the value for a rounded entrance can be as low as 0.1. Our water flow data give a mean value of  $K_{\text{contr.}} = 0.23$ , which is evidently the same as the high-Reynolds number asymptote for all data on suspensions as shown in the logarithmic plot in figure 11. It appears from this plot that the data in the low-Reynolds number range, though somewhat sparse, follow the same sort of Reynolds number dependence as that of  $K$  for laminar flow through bends. The transition from laminar to turbulent regimes takes place at about  $Re_m \sim 3900$ , although the range between about  $4 \times 10^3$  and  $1 \times 10^5$  may well represent a transition region. The relationships for laminar and turbulent flow through a contraction are given by

$$K_{\text{contr. (L)}} = 900/Re_m \quad \text{for } Re_m \leq 3900 \quad [35]$$

$$K_{\text{contr. (T)}} = \bar{K}_{\text{contr.}\infty} = 0.23 \quad \text{for } Re_m > 3900. \quad [36]$$

For the sudden enlargement [1] gives

$$K_{\text{expn.}} = [h_f/(V_1^2/2)] = [-\Delta P/(\rho V_1^2/2)] + (1 - \beta^4) \quad [37]$$

in which  $\beta = (D_1/D_2) < 1$ . For our  $2.5 \times 5.0 \text{ cm}^2$  ( $1 \times 2 \text{ in}^2$  standard pipe) concentric expansion  $\beta = 0.5075$ . For turbulent Newtonian flow through a sudden expansion, one can derive the approximate relation (Bird *et al.* 1960, p. 219)

$$K_{\text{expn. (T)}} = h_f/(V_1^2/2) \approx (1 - \beta^2)^2. \quad [38]$$



For Newtonian flow through our  $2.5 \times 5.0 \text{ cm}^2$  test expansion [38] gives  $K_{\text{expn. (T)}} = 0.5512$ . The experimental  $K_{\text{expn.}}$  values, constituting a total of 152 data points, are given in the plot against  $\text{Re}_m$  in figure 12. The solid curve in this plot has the equation

$$K_{\text{expn.}} = 115.1/\text{Re}_m + (1 - \beta^2)^2. \quad [39]$$

From the plot in figure 12 it is somewhat difficult to ascertain the value of  $\text{Re}_m$  for which the first, laminar flow term in [39] becomes negligible in comparison with the turbulent flow term. However, the first term on the right-hand side of the equation is about 5% of the turbulent flow term,  $(1 - \beta^2)^2 = 0.5512$ , when  $\text{Re}_m \sim 4180$ .

### 2.5. Flow of non-Newtonian suspensions through Venturi meters

Flow rates of water and non-Newtonian suspensions through 2.5 and 5.0 cm Venturi meters with throat to pipe diameter ratios of 0.50 and 0.75 were measured over a broad range of Reynolds numbers. Because the main interest is with suspension systems, which often have varying tendencies to settle, we ran experiments with the Venturi meters installed in a vertical orientation with the flow directed upwards. Such an arrangement is most suitable for highly settling, coarse particle slurry flows (Turian *et al.* 1983). As a check, we also ran experiments on the flow of the 5.7 and 8.3 vol.% laterite suspensions through the 5.0 cm Venturi meter with  $\beta = 0.75$  in a horizontal orientation, partly because we had obtained discharge coefficients exceeding 1 with this device installed in the vertical orientation. We found no discernible difference in the data that could be attributed to orientation, as discharge coefficients exceeding 1 were obtained regardless of the orientation of the meter. This finding is not new. It may be a manifestation of drag reduction, though this has not been definitively established. The discharge coefficient for flow through a horizontally-oriented Venturi meter is defined by [20] in which, as usual, subscript 1 refers to the inlet section and subscript 2 refers to the Venturi throat. The only modification needed for a vertically-oriented Venturi meter with the flow in the upward direction is to replace  $(P_1 - P_2) = -\Delta P$  by  $(\tilde{P}_1 - \tilde{P}_2) = (P_1 - P_2) - (\rho g \Delta Z)$  in [20]. Note that  $\Delta Z = (Z_2 - Z_1) > 0$  since the flow is in the upward direction.

For Newtonian fluids it is known that Venturi meters are most suitable for fully-developed turbulent flow, when the discharge coefficient approaches a constant asymptotic value, usually about  $C_v \sim 0.95-1.0$ . The value of the discharge coefficient depends upon the particular design of the Venturi meter. The devices used in our studies were purchased ready-made, of stainless steel construction, having a special commercial design aimed at minimizing overall length. They are strictly suitable for turbulent flow service. Figure 13 provides a schematic diagram and detailed dimensions of the commercial Venturi meters used in our studies.

Figures 14 and 15 provide plots of the experimental discharge coefficients against Reynolds number for the flow of water and the laterite and gypsum suspensions for the 1 and 5.0 cm Venturi meters, respectively. Table 9 lists the asymptotic mean values of the discharge coefficients,  $\bar{C}_v$ , their variation or range about this mean and the transition Reynolds number delineating the turbulent flow regime.

## 3. CONCLUSIONS

The principal results in this work include the finding that the resistance coefficients for non-Newtonian suspension flow through bends of various angles and radii of curvature, and through valves decrease with increasing Reynolds number in the laminar flow regime. Resistance coefficient values for laminar flow which included the friction loss contribution attributable to the length of the fitting,  $K_{(L)}$ , were found in general to be inversely proportional to the generalized Reynolds number. The dependence for the corresponding coefficients,  $K_{\text{excl. (L)}}$ , excluding the contribution equivalent to the loss for fully-developed flow through a straight pipe having the same length as the physical length of the fitting were also in general found to vary inversely with Reynolds number, but to a somewhat smaller power than 1. The two resistance coefficients are related by [26]. If we combine [30] and [26], and use  $f = 16/\text{Re}_m$  for fully-developed, laminar suspension flow through a straight pipe, we formally get

$$K_{\text{excl. (L)}} = [A - 64(L_f/D)]/\text{Re}_m. \quad [40]$$

The form of [40] for bends of bend angle  $\Theta$  radians is obtained from [13] as

$$K_{\text{excl. (L)}} = [A - 64(r_c \Theta / D)] / \text{Re}_m. \quad [41]$$

Accordingly, [40] and [41] could be used as alternatives to [26]. The power  $\lambda$  in [26] is generally less than unity as it is obtained by a complete refitting of the  $K_{\text{excl. (L)}}$  vs  $\text{Re}_m$  data. In the present work we used [25] directly to determine  $K_{\text{excl.}}$ , using the experimentally measured pressure gradient,  $(-\Delta P/L)_s$ , for flow in a straight pipe of the same diameter and material as the fitting.

The two coefficients,  $K$  and  $K_{\text{excl.}}$ , are equal for the mitre bend since  $r_c = 0$ . It was indicated earlier, in reference to [30] and table 5, that we could not obtain data in the laminar flow regime for this high-loss bend. In fact the  $K$  values for this fitting over the lower Reynolds number range, before the asymptotic value for fully-developed turbulent flow had been attained, did decrease with increasing Reynolds number, but at a much slower rate than to the inverse power given by [41]. This suggests that this lower Reynolds number range corresponds to a transition region between fully laminar and fully turbulent flows. Indeed, the difference in the dependence given by [32] and that in [40] or [41] may well be due to the fact that the lower Reynolds number ranges to which these laminar-flow resistance coefficients belong includes a transition region. Clearly, the values of the coefficients  $K_{\text{excl. (L)}}$  would be more sensitive to the existence of a transition region. We view the correlation forms given by [30] and [32] as useful approximations. Their further refinement would require flow data using precisely designed and fabricated bends and fittings, although such model experimental devices have little practical relevance. Considering the variability in design of commercially available flow devices, and the fact that resistance coefficients for laminar flow through fittings are not usually called for, the approximations presented in this work are not only quite adequate, they are very useful.

The finding that the resistance coefficients for all the bends, the valves and the sudden contraction and expansion, and additionally the finding also that the discharge coefficients for all the Venturi meters, in fully-developed turbulent flow, all approach constant asymptotic values which are the same as for the corresponding coefficients for flow of water is very significant. It is because this means one can establish the turbulent-flow friction-loss characteristic for any flow element using data with water. Then, one only need use the density of the suspension to calculate the applicable friction loss. It has been observed earlier that bend, fitting and valve designs vary with manufacturer and with size. Therefore, individual determination of loss characteristics is often inevitable.

The existence of high-Reynolds number asymptotic values of resistance coefficient is due to the fact that inertial forces predominate over other forces in the fully turbulent flow regime. Indeed, inertial effects turn out to be more prominent for flow through complex geometries than for the straight pipe (Turian *et al.* 1997) because of enhanced turbulence. The findings in the present work confirm for non-Newtonian suspensions what we had also discovered earlier in relation to heterogeneous, dense- and/or coarse-particle slurries (Turian *et al.* 1983). These heterogeneous slurries were not amenable to rheological characterization; they settled too fast. Furthermore, we could not get friction-loss data in the laminar flow regime with these dense/coarse-particle slurries, as excessive settling led to unsteady conditions.

## REFERENCES

- Adler, M. (1934) Stromung in gekrummen Rohren. *Z. Angew. Math. Mech.* **14**, 257–275.
- Barua, S. N. (1963) On the secondary flow in stationary curved pipe. *Quart. J. Mech. Appl. Math.* **16**, 61–77.
- Benedict, R. P. (1977) *Fundamentals of Temperature, Pressure, and Flow Measurements* 2nd edn. John Wiley, New York.
- Benedict, R. P. (1980) *Fundamentals of Pipe Flow*. John Wiley, New York.
- Bird, R. B., Stewart, W. E. and Lightfoot, E. N. (1960) *Transport Phenomena*. John Wiley, New York.
- Boger, D. V., Gupta, R. and Tanner, R. I. (1978) The end correction for power-law fluids in the capillary rheometer. *J. non-Newtonian Fluid Mech.* **4**, 239–248.
- Brook, N. (1962) Flow measurement of solid–liquid mixtures using Venturi and other meters. *Proc. Inst. Mech. Eng.* **176**, 127–140.

- Collins, W. M. and Dennis, S. C. R. (1975) The steady motion of a viscous fluid in a curved tube. *Quart. J. Mech. Appl. Math.* **28**, 133–156.
- Crane Company (1980) Flow of fluids through valves, fittings and pipe. Tech. Paper No. 410, Crane Co., 300 Park Avenue, New York.
- Dean, W. R. (1927) Note on the motion of a fluid in a curved pipe. *Philos. Mag., Ser. 7* **4**, 208–233.
- Dean, W. R. (1928) The streamline motion of a fluid in a curved pipe. *Philos. Mag., Ser. 7* **5**, 673–695.
- Halmos, A. L., Boger, D. V. and Cabelli, A. (1975) The behavior of a power-law fluid flowing through a sudden expansion: Part I. A numerical solution; Part II. Experimental verification. *AIChE J.* **21**, 540–553.
- Hanson, R. D., Barian, D. and Chaudhry, N. (1982) Lignite–water slurry flow measurement using a Venturi meter. *Symp. on Instrumentation and Control for Fossil Energy Processes*, pp. 458–464.
- Harris, J. and Magnall, A. N. (1972) The use of orifice plates and Venturi meters with non-Newtonian fluid. *Trans. Inst. Chem. Eng.* **50**, 61–68.
- Herringe, R. A. (1977) Slurry flow metering by pressure differential devices. *Int. J. Multiphase Flow* **3**, 285–298.
- Hooper, W. B. (1981) The two- $K$  method predicts head losses in pipe fittings. *Chemical Eng.* August, 96–100.
- Ito, H. (1959) Pressure losses in smooth pipe bends. *J. Basic Eng., Trans. ASME, Ser. D* **81**, 123–134.
- Ito, H. (1960) Friction factors for turbulent flow in curved pipes. *J. Basic Eng., Trans. ASME, Ser. D* **82**, 131–145.
- Ito, H. (1969) Laminar flow in curved pipes. *Z. Angew. Math. Mech.* **49**, 653–663.
- Keulegan, G. H. and Beij, K. H. (1937) Pressure losses for fluid flow in pipes. *J. Research Nat. Bur. Standards* **18**, 89–114.
- Ma, T.-W. (1987) Stability, rheology and flow in pipes, bends, fittings, valves and Venturi meters of concentrated non-Newtonian suspensions. Ph.D. Thesis, University of Illinois at Chicago, Chicago, IL, U.S.A.
- Macagno, E. O. and Hung, T. K. (1967) Computational and experimental study of a captive annular eddy. *J. Fluid Mech.* **28**, 43–64.
- Mori, Y. and Nakayama, W. (1965) Study on forced convective heat transfer in curved pipes. First Report: Laminar region. *Int. J. Heat Mass Transfer* **8**, 67–82.
- Mukhtar, A., Singh, S. N. and Seshadri, V. (1995) Pressure drop in a long radius 90° horizontal bend for the flow of multisized heterogeneous slurries. *Int. J. Multiphase Flow* **21**, 329–334.
- Shook, C. A. and Masliyah, J. H. (1974) Flow of slurry through a Venturi meter. *Can. J. Chem. Eng.* **52**, 228–233.
- Turian, R. M., Hsu, F. L. and Selim, M. S. (1983) Friction losses for flow of slurries in pipeline bends, fittings and valves. *Int. J. Particulate Science and Technology* **1**, 365–392.
- Turian, R. M., Ma, T.-W., Hsu, F.-L. G. and Sung, D.-J. (1998) Flow of concentrated non-Newtonian slurries: 1. Friction losses in laminar, turbulent and transition flow through straight pipe. *Int. J. Multiphase Flow*, **24**, 225–241.
- van Dyke, M. (1978) Extended Stokes series: laminar flow through a loosely coiled pipe. *J. Fluid Mech.* **86**, 129–145.
- Ward-Smith, A. J. (1980) *Internal Fluid Flow: The Fluid Dynamics of Flow in Pipes and Ducts*. Oxford University Press, New York.
- White, C. M. (1929) Streamline flow through curved pipes. *Proc. Roy. Soc.* **A123**, 645–663.